

1 **Disentangling Sources of Gene Tree Discordance in Phylogenomic Datasets: Testing**

2 **Ancient Hybridizations in Amaranthaceae s.l.**

3

4 Diego F. Morales-Briones<sup>1\*</sup>, Gudrun Kadereit<sup>2</sup>, Delphine T. Tefarikis<sup>2</sup>, Michael J. Moore<sup>3</sup>,

5 Stephen A. Smith<sup>4</sup>, Samuel F. Brockington<sup>5</sup>, Alfonso Timoneda<sup>5</sup>, Won C. Yim<sup>6</sup>, John C.

6 Cushman<sup>6</sup>, Ya Yang<sup>1\*</sup>

7

8 <sup>1</sup> Department of Plant and Microbial Biology, University of Minnesota-Twin Cities, 1445

9 Gortner Avenue, St. Paul, MN 55108, USA

10 <sup>2</sup> Institut für Molekulare Physiologie, Johannes Gutenberg-Universität Mainz, D-55099, Mainz,

11 Germany

12 <sup>3</sup> Department of Biology, Oberlin College, Science Center K111, 119 Woodland Street, Oberlin,

13 OH 44074-1097, USA

14 <sup>4</sup> Department of Ecology & Evolutionary Biology, University of Michigan, 830 North University

15 Avenue, Ann Arbor, MI 48109-1048, USA

16 <sup>5</sup> Department of Plant Sciences, University of Cambridge, Tennis Court Road, Cambridge, CB2

17 3EA, United Kingdom

18 <sup>6</sup> Department of Biochemistry and Molecular Biology, University of Nevada, Reno, NV, 89577,

19 USA

20

21 \* Correspondence to be sent to: Diego F. Morales-Briones and Ya Yang. Department of Plant and

22 Microbial Biology, University of Minnesota, 1445 Gortner Avenue, St. Paul, MN 55108, USA,

23 Telephone: +1 612-625-6292 (YY) Email: [dfmoralesb@gmail.com](mailto:dfmoralesb@gmail.com); [yangya@umn.edu](mailto:yangya@umn.edu)

24 **Abstract.** — Gene tree discordance in large genomic datasets can be caused by evolutionary  
25 processes such as incomplete lineage sorting and hybridization, as well as model violation, and  
26 errors in data processing, orthology inference, and gene tree estimation. Species tree methods  
27 that identify and accommodate all sources of conflict are not available, but a combination of  
28 multiple approaches can help tease apart alternative sources of conflict. Here, using a  
29 phylotranscriptomic analysis in combination with reference genomes, we test a hypothesis of  
30 ancient hybridization events within the plant family Amaranthaceae s.l. that was previously  
31 supported by morphological, ecological, and Sanger-based molecular data. The dataset included  
32 seven genomes and 88 transcriptomes, 17 generated for this study. We examined gene-tree  
33 discordance using coalescent-based species trees and network inference, gene tree discordance  
34 analyses, site pattern tests of introgression, topology tests, synteny analyses, and simulations. We  
35 found that a combination of processes might have generated the high levels of gene tree  
36 discordance in the backbone of Amaranthaceae s.l. Furthermore, we found evidence that three  
37 consecutive short internal branches produce anomalous trees contributing to the discordance.  
38 Overall, our results suggest that Amaranthaceae s.l. might be a product of an ancient and rapid  
39 lineage diversification, and remains, and probably will remain, unresolved. This work highlights  
40 the potential problems of identifiability associated with the sources of gene tree discordance  
41 including, in particular, phylogenetic network methods. Our results also demonstrate the  
42 importance of thoroughly testing for multiple sources of conflict in phylogenomic analyses,  
43 especially in the context of ancient, rapid radiations. We provide several recommendations for  
44 exploring conflicting signals in such situations.

45 **Keywords:** Amaranthaceae; gene tree discordance; hybridization; incomplete lineage sorting;  
46 phylogenomics; transcriptomics; species tree; species network.

47 The exploration of gene tree discordance has become common in the phylogenetic era (Salichos  
48 et al. 2014; Smith et al. 2015; Huang et al. 2016; Pease et al. 2018) and is essential for  
49 understanding the underlying processes that shape the Tree of Life. Discordance among gene  
50 trees can be the product of multiple sources. These include errors and noise in data assembly and  
51 filtering, hidden paralogy, incomplete lineage sorting (ILS), gene duplication/loss (Pamilo and  
52 Nei 1988; Doyle 1992; Maddison 1997; Galtier and Daubin 2008), random noise from  
53 uninformative genes, as well as misspecified model parameters of molecular evolution such as  
54 substitutional saturation, codon usage bias, or compositional heterogeneity (Foster 2004; Cooper  
55 2014; Cox et al. 2014; Liu et al. 2014). Among these potential sources of gene tree discordance,  
56 ILS is the most studied in the systematics literature (Edwards 2009), and several phylogenetic  
57 inference methods have been developed to accommodate ILS as the source of discordance  
58 (reviewed in Edwards et al. 2016; Mirarab et al. 2016; Xu and Yang 2016). More recently,  
59 methods that account for additional processes such as hybridization or introgression have gained  
60 attention. These include methods that estimate phylogenetic networks while accounting for ILS  
61 and hybridization simultaneously (e.g., Solís-Lemus and Ané 2016; Wen et al. 2018), and  
62 methods that detect introgression based on site patterns or phylogenetic invariants (e.g., Green et  
63 al. 2010; Durand et al. 2011; Kubatko and Chifman 2019). Frequently, multiple processes can  
64 contribute to gene tree heterogeneity (Holder et al. 2001; Buckley et al. 2006; Meyer et al. 2017;  
65 Knowles et al. 2018). However, at present, no method can estimate species trees from  
66 phylogenomic data while modeling multiple sources of conflict and heterogeneity in molecular  
67 substitution simultaneously. To overcome these limitations, the use of multiple phylogenetic  
68 tools and data partitioning schemes in phylogenomic datasets is essential to disentangle sources  
69 of gene tree heterogeneity and resolve recalcitrant relationships at deep and shallow nodes of the

70 Tree of Life (e.g., Alda et al. 2019; Widhelm et al. 2019; Prasanna et al. 2020; Roycroft et al.  
71 2020).

72 In this study, we evaluate multiple sources of gene tree conflict to test controversial  
73 hypotheses of ancient hybridization among subfamilies in the plant family Amaranthaceae s.l.  
74 Amaranthaceae s.l. includes the previously segregated family Chenopodiaceae (Hernández-  
75 Ledesma et al. 2015; The Angiosperm Phylogeny Group 2016). With ca. 2050 to 2500 species in  
76 181 genera and a worldwide distribution (Hernández-Ledesma et al. 2015), Amaranthaceae s.l. is  
77 iconic for the repeated evolution of complex traits representing adaptations to extreme  
78 environments such as C<sub>4</sub> photosynthesis in hot and often dry environments (e.g., Kadereit et al.  
79 2012; Bena et al. 2017), various modes of extreme salt tolerance (e.g., Flowers and Colmer 2015;  
80 Piirainen et al. 2017) that in several species are coupled with heavy metal tolerance (Moray et al.  
81 2016), and very fast seed germination and production of multiple diaspore types on one  
82 individual (Kadereit et al. 2017). Several important crops are members of Amaranthaceae s.l.,  
83 such as the pseudocereals quinoa and amaranth, sugar beet, spinach, glassworts, and saltworts.  
84 Many species of the family are also important fodder plants in arid regions and several are  
85 currently being investigated for their soil remediating and desalinating effects (e.g., Li et al.  
86 2019). Due to their economic importance, reference genomes are available for *Beta vulgaris*  
87 (sugar beet, subfamily Betoideae; Dohm et al. 2014), *Chenopodium quinoa* (quinoa,  
88 Chenopodioideae; Jarvis et al. 2017), *Spinacia oleracea* (spinach; Chenopodioideae; Xu et al.  
89 2017) and *Amaranthus hypochondriacus* (amaranth; Amaranthoideae; Lightfoot et al. 2017),  
90 representing three of the 13 currently recognized subfamilies of Amaranthaceae s.l. (sensu  
91 Kadereit et al. 2003; Kadereit et al. 2017).

92           Within the core Caryophyllales the previously segregated families Amaranthaceae s.s.  
93   and Chenopodiaceae have always been regarded as closely related, and their separate family  
94   status has long been the subject of phylogenetic and taxonomic debate (Kadereit et al. 2003;  
95   Masson and Kadereit 2013; Hernández-Ledesma et al. 2015; Walker et al. 2018; Fig. 1). Their  
96   close affinity is supported by a number of shared morphological, anatomical and phytochemical  
97   synapomorphies, and has been substantiated by molecular phylogenetic studies (discussed in  
98   Kadereit et al. 2003). Amaranthaceae s.s. has a predominantly tropical and subtropical  
99   distribution with the highest diversity found in the Neotropics, eastern and southern Africa and  
100   Australia (Müller and Borsch 2005), while Chenopodiaceae predominantly occurs in temperate  
101   regions and semi-arid or arid environments of subtropical regions (Kadereit et al. 2003). The key  
102   problem has always been the species-poor and heterogeneous subfamilies Polycnemoideae and  
103   Betoideae, neither of which fit easily within Chenopodiaceae or Amaranthaceae s.s. (cf. Table 5  
104   in Kadereit et al. 2003). Polycnemoideae is similar in ecology and distribution to  
105   Chenopodiaceae but shares important floral traits such as petaloid tepals, filament tubes and 2-  
106   locular anthers with Amaranthaceae s.s. Morphologically, Betoideae fits into either  
107   Chenopodiaceae or Amaranthaceae s.s. but has a unique fruit type—a capsule that opens with a  
108   circumscissile lid (Kadereit et al. 2006). Both Betoideae and Polycnemoideae possess only a few  
109   species each and each has a strongly disjunct distribution pattern across three continents.  
110   Furthermore, the genera of both subfamilies display a number of morphologically dissociating  
111   features. Both intercontinental disjunctions of species-poor genera and unique or intermediate  
112   morphological traits led to the hypothesis that Betoideae and Polycnemoideae might have  
113   originated from hybridization events among early-branching lineages in Amaranthaceae s.l.  
114   (Hohmann et al. 2006; Masson and Kadereit 2013). To test this hypothesis, a

115 phylotranscriptomic approach is particularly compelling as it not only provides thousands of  
116 low-copy nuclear genes for dissecting sources of phylogenetic discordance, but also enables  
117 future studies associating gene tree topology with gene function and habitat adaptation.

118         Previous molecular phylogenetic analyses struggled to resolve the relationships among  
119 Betoideae, Polycnemoideae and the rest of the Amaranthaceae s.l. (Fig. 1). The first  
120 phylogenomic study of Amaranthaceae s.l. using nuclear loci (Walker et al. 2018; Fig. 1e)  
121 revealed that gene tree discordance mainly occurred at deep nodes of the phylogeny involving  
122 Betoideae. Polycnemoideae was sister to Chenopodiaceae, albeit supported by only 17% of gene  
123 trees, which contradicted previous analyses based on plastid data (Fig. 1, a–d). However, only a  
124 single species of Betoideae (the cultivated beet and its wild relative) was sampled in Walker et  
125 al. (2018). Furthermore, Walker et al. (2018) found conflicting topologies between concatenated  
126 and coalescent-based analyses, but sources of conflicting signals among gene trees remained  
127 unexplored.

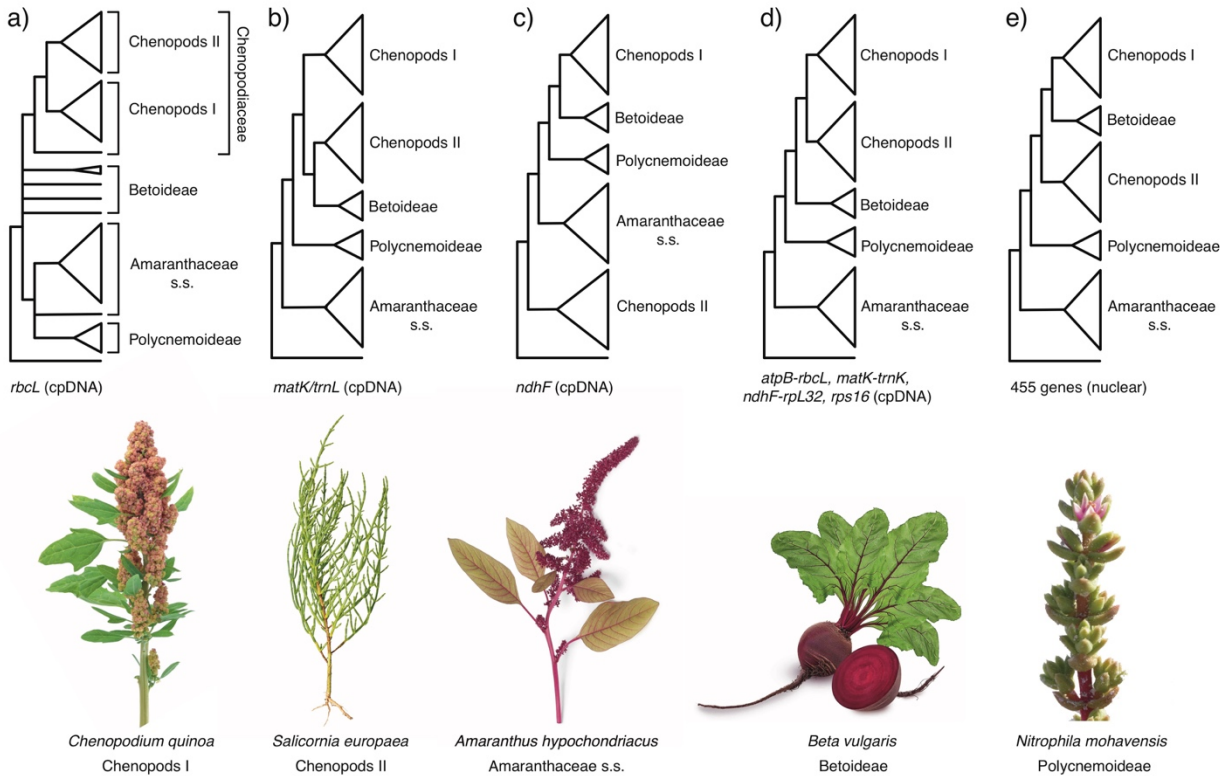
128         In this study, we used a large genomic dataset to examine sources of gene tree  
129 discordance in Amaranthaceae s.l. Specifically, we tested whether Polycnemoideae and  
130 Betoideae result from independent hybridizations between Amaranthaceae s.s. and  
131 Chenopodioideae by distinguishing the signal of hybridization from gene tree discordance  
132 produced by ILS, uninformative gene trees, hidden paralogy, misspecifications of model of  
133 molecular evolution, and hard polytomy.

134

135

136

137



138

139 **FIGURE 1.** Phylogenetic hypothesis of Amaranthaceae s.l. from previous studies. a) Kadereit et  
140 al. (2003) using the plastid (cpDNA) *rbcL* coding region. b) Müller and Borsch (2005); using the  
141 cpDNA *matK* coding region and partial *trnL* intron. c) Hohmann et al. (2006) using the cpDNA  
142 *ndhF* coding region. d) Kadereit et al. (2017) using the cpDNA *atpB-rbcL* spacer, *matK* with  
143 *trnL* intron, *ndhF-rpL32* spacer, and *rps16* intron e) Walker et al. (2018) using 455 nuclear genes  
144 from transcriptome data. Major clades of Amaranthaceae s.l. named following the results of this  
145 study. Image credits: *Amaranthus hypochondriacus* by Picture Partners, *Beta vulgaris* by Olha  
146 Huchek, *Chenopodium quinoa* by Diana Mower, *Nitrophila mohavensis* by James M. André, and  
147 *Salsola soda* by Homeydesign.

148

149

## MATERIALS AND METHODS

150 An overview of all dataset and phylogenetic analyses can be found in Figure S1.

151

152 *Taxon sampling, transcriptome sequencing*

153 We sampled 92 ingroup species (88 transcriptomes and four genomes) representing 53 genera  
154 (out of ca. 181) of all 13 currently recognized subfamilies and 16 out of 17 tribes of  
155 Amaranthaceae s.l. (sensu [Kadereit et al. 2003; Kadereit et al. 2017]). In addition, 13 outgroups  
156 across the Caryophyllales were included (ten transcriptomes and three genomes; Table S1). We  
157 generated 17 new transcriptomes for this study on an Illumina HiSeq2500 platform (Table S2).  
158 Library preparation was carried out using either poly-A enrichment or ribosomal RNA depletion.  
159 See Supplemental Methods for details on tissue collection, RNA isolation, library preparation,  
160 and quality control.

161

162 *Transcriptome data processing, assembly, homology and orthology inference*

163 Read processing, assembly, translation, and homology and orthology inference followed the  
164 ‘phylogenomic dataset construction’ pipeline (Yang and Smith 2014) with multiple updates. We  
165 briefly describe our procedure below, with details in the Supplemental Methods and updated  
166 scripts in [https://bitbucket.org/yanglab/phylogenomic\\_dataset\\_construction/](https://bitbucket.org/yanglab/phylogenomic_dataset_construction/)

167 We processed raw reads for all 88 transcriptome datasets (except *Bienertia sinuspersici*)  
168 used in this study (Table S1). Reads were corrected for errors, trimmed for sequencing adapters  
169 and low-quality bases, and filtered for organellar reads. *De novo* assembly of processed nuclear  
170 reads was carried out with Trinity v 2.5.1 (Grabherr et al. 2011) with default settings, but without  
171 *in silico* normalization. Low-quality and chimeric transcripts were removed. Filtered transcripts  
172 were clustered into putative genes with Corset v 1.07 (Davidson and Oshlack 2014) and only the  
173 longest transcript of each putative gene was retained (Chen et al. 2019). Lastly, transcripts were  
174 translated, and identical coding sequences (CDS) were removed. Homology inference was



175 carried out on CDS using reciprocal BLASTN, followed by orthology inference using the  
176 ‘monophyletic outgroup’ approach (Yang and Smith 2014), keeping only ortholog groups with at  
177 least 25 ingroup taxa.

178

179 *Assessment of recombination*

180 Coalescent species tree methods assume that there is free recombination between loci and no  
181 recombination within loci. To determine the presence of recombination in our dataset, we used  
182 the pairwise homoplasy index test  $\Phi$  for recombination, as implemented in PhiPack (Bruen et al.  
183 2006). We tested recombination on the final set of ortholog alignments (with a minimum of 25  
184 taxa) with the default sliding window size of 100 bp. Alignments that showed a strong signal of  
185 recombination with  $p \leq 0.05$  were removed from all subsequent phylogenetic analyses.

186

187 *Nuclear phylogenetic analysis*

188 We used both concatenation and coalescent-based methods to reconstruct the phylogeny of  
189 Amaranthaceae s.l. Sequences from final orthologs were aligned using MAFFT v 7.307 (Katoh  
190 and Standley 2013) with settings ‘—genafpair --maxiterate 1000’. Columns with more than 70%  
191 missing data were trimmed with Phyx (Brown et al. 2017), and alignments with at least 1,000  
192 characters and 99 out of 105 taxa were retained. We first estimated a maximum likelihood (ML)  
193 tree of the concatenated matrix with RAxML v 8.2.11 (Stamatakis 2014) using a partition-by-  
194 gene scheme with GTRCAT model for each partition and clade support assessed with 200 rapid  
195 bootstrap (BS) replicates. To estimate a coalescent-based species tree, first we inferred individual  
196 ML gene trees using RAxML with a GTRCAT model and 200 BS replicates to assess clade  
197 support. Gene trees were then used to infer a species tree with ASTRAL-III v5.6.3 (Zhang et al.

198 2018) using local posterior probabilities (LPP; Sayyari and Mirarab 2016) to assess clade  
199 support.

200

201 *Detecting and visualizing nuclear gene tree discordance*

202 To explore discordance among gene trees, we first calculated the internode certainty all (ICA)  
203 value to quantify the degree of conflict on each node of a target tree (i.e., species tree) given  
204 individual gene trees (Salichos et al. 2014). In addition, we calculated the number of conflicting  
205 and concordant bipartitions on each node of the species trees. Both the ICA scores and  
206 conflicting/concordant bipartitions were calculated with Phyparts (Smith et al. 2015), mapping  
207 against the inferred ASTRAL species trees, using individual gene trees with BS support of at  
208 least 50% for the corresponding node. Additionally, in order to distinguish strong conflict from  
209 weakly supported branches, we carried out Quartet Sampling (QS; Pease et al. 2018) with 100  
210 replicates. Quartet Sampling subsamples quartets from the input tree and alignment and assesses  
211 the confidence, consistency, and informativeness of each internal branch by the relative  
212 frequency of the three possible quartet topologies (Pease et al. 2018). Both ICA and Quartet  
213 Sampling scores provide an alternative branch support that reflects underlying gene tree conflict  
214 and that is not affected by anomalous high levels of bootstrap support common in phylogenomic  
215 data (Kumar et al. 2012).

216 To further visualize conflict, we built a cloudogram using DensiTree v2.2.6 (Bouckaert  
217 and Heled 2014). As DensiTree cannot accommodate missing taxa among gene trees, we  
218 reduced the final ortholog alignments to include 41 species (38 ingroup and 3 outgroups) in order  
219 to include as many orthologs as possible while representing all main clades of Amaranthaceae  
220 s.l. (see results). Individual gene trees were inferred as previously described. Trees were time-

221 calibrated with TreePL v1.0 (Smith and O’Meara 2012) by fixing the crown age of  
222 Amaranthaceae s.l. to 66–72.1 based on a pollen record of *Polyporina cribraria* from the late  
223 Cretaceous (Maastrichtian; Srivastava 1969), and the root for the reduced 41-species dataset  
224 (most common recent ancestor of Achatocarpaceae and Aizoaceae) was set to 95 Ma based on  
225 the time-calibrated plastid phylogeny of Caryophyllales from Yao et al. (2019).

226

227 *Plastid assembly and phylogenetic analysis*

228 Although DNase treatment was carried out to remove genomic DNA, due to their high copy  
229 number, plastid sequences are often carried over in RNA-seq libraries. In addition, as young leaf  
230 tissue was used for RNA-seq, the presence of RNA from plastid genes is expected to be  
231 represented. To investigate phylogenetic signal from plastid sequences, *de novo* assemblies were  
232 carried out with the Fast-Plast v.1.2.6 pipeline (<https://github.com/mrmckain/Fast-Plast>) using  
233 the filtered organelle reads. Contigs produced by Spades v 3.9.0 (Bankevich et al. 2012) were  
234 mapped to the closest available reference plastomes (Table S3), one copy of the Inverted Repeat  
235 was removed, and the remaining contigs manually edited in Geneious v.11.1.5 (Kearse et al.  
236 2012) to produce the final oriented contigs.

237 Contigs were aligned with MAFFT with the setting ‘--auto’. Two samples (*Dysphania*  
238 *schraderiana* and *Spinacia turkestanica*) were removed due to low sequence occupancy. Using  
239 the annotations of the reference genomes (Table S3), the coding regions of 78 genes were  
240 extracted and each gene alignment was visually inspected in Geneious to check for potential  
241 misassemblies. From each gene alignment, taxa with short sequences (i.e., < 50% of the aligned  
242 length) were removed and the remaining sequences realigned with MAFFT. The genes *rpl32* and  
243 *ycf2* were excluded from downstream analyses due to low taxon occupancy (Table S4). For each

244 individual gene we performed extended model selection (Kalyaanamoorthy et al. 2017) followed  
245 by ML gene tree inference and 1,000 ultrafast bootstrap replicates for branch support (Hoang and  
246 Chernomor 2018) in IQ-TREE v.1.6.1 (Nguyen et al. 2015). For the concatenated matrix we  
247 searched for the best partition scheme (Lanfear et al. 2012) followed by ML gene tree inference  
248 and 1,000 ultrafast bootstrap replicates for branch support in IQ-Tree. Additionally, we evaluated  
249 branch support with QS using 1,000 replicates and gene tree discordance with PhyParts. Lastly,  
250 to identify the origin of the plastid reads (i.e., genomic or RNA), we predicted RNA editing from  
251 CDS alignments using PREP (Mower 2009) with the alignment mode (PREP-aln), and a cutoff  
252 value of 0.8.

253

254 *Species network analysis using a reduced 11-taxon dataset*

255 We inferred species networks that model ILS and gene flow using a maximum pseudo-likelihood  
256 approach (Yu and Nakhleh 2015). Species network searches were carried out with PhyloNet  
257 v.3.6.9 (Than et al. 2008) with the command ‘InferNetwork\_MPL’ and using the individual gene  
258 trees as input. Due to computational restrictions, and given our main focus to identify potential  
259 reticulating events among major clades of Amaranthaceae s.l., we reduced our taxon sampling to  
260 one outgroup and ten ingroup taxa to include two representative species from each of the five  
261 well-supported major lineages in Amaranthaceae s.l. (see results). We filtered the final 105-taxon  
262 ortholog set to include genes that have all 11 taxa [referred herein as 11-taxon(net) dataset; Fig  
263 S1.]. After alignment and trimming we kept genes with a minimum of 1,000 aligned base pairs  
264 and individual ML gene trees were inferred using RAxML with a GTRGAMMA model and 200  
265 bootstrap replicates. We carried out five network searches by allowing one to five reticulation  
266 events and ten runs for each search. To estimate the optimum number of reticulations, we

267 optimized the branch lengths and inheritance probabilities and computed the likelihood of the  
268 best scored network from each of the five maximum reticulation events searches. Network  
269 likelihoods were estimated given the individual gene trees using the command ‘CalGTProb’ in  
270 PhyloNet (Yu et al. 2012). Then, we performed model selection using the bias-corrected Akaike  
271 information criterion (AICc; Sugiura 1978), and the Bayesian information criterion (BIC;  
272 Schwarz 1978). The number of parameters was set to the number of branch lengths being  
273 estimated plus the number of hybridization probabilities being estimated. The number of gene  
274 trees used to estimate the likelihood was used to correct for finite sample size. To compare  
275 network models to bifurcating trees, we also estimated bifurcating concatenated ML and  
276 coalescent-based species trees and a plastid tree as previously described with the reduced 11-  
277 species taxon sampling.

278

279 *Hypothesis testing and detecting introgression using four-taxon datasets*

280 Given the signal of multiple clades potentially involved in hybridization events detected by  
281 PhyloNet (see results), we next conducted quartet analyses to explore a single event at a time.  
282 First, we further reduced the 11-taxon(net) dataset to six taxa that included one outgroup genome  
283 (*Mesembryanthemum crystallinum*) and one ingroup from each of the five major ingroup clades:  
284 *Amaranthus hypochondriacus* (genome), *Beta vulgaris* (genome), *Chenopodium quinoa*  
285 (genome), *Caroxylon vermiculatum* (transcriptome), and *Polycnemum majus* (transcriptome) to  
286 represent Amaranthaceae s.s., Betoideae, 'Chenopods I', 'Chenopods II' and Polycnemoideae,  
287 respectively. We carried out a total of ten quartet analyses using all ten four-taxon combinations  
288 that included three out of five ingroup species and one outgroup. We filtered the final set of 105-  
289 taxon orthologs for genes with all four taxa for each combination and inferred individual gene

290 trees as described before. For each quartet we carried out the following analyses. We first  
291 estimated a species tree with ASTRAL and explored gene tree conflict with PhyParts. We then  
292 explored individual gene tree resolution by calculating the Tree Certainty (TC) score (Salichos et  
293 al. 2014) in RAxML using the majority rule consensus tree across the 200 bootstrap replicates.  
294 Next, we explored potential correlation between TC score and alignment length, GC content and  
295 alignment gap proportion using a linear regression model in R v.3.6.1 (R Core Team 2019).  
296 Lastly, we tested for the fit of gene trees to the three possible rooted quartet topologies for each  
297 gene using the approximately unbiased (AU) tests (Shimodaira 2002). We carried out ten  
298 constraint searches for each of three topologies in RAxML with the GTRGAMMA model, then  
299 calculated site-wise log-likelihood scores for the three constraint topologies in RAxML using  
300 GTRGAMMA and carried out the AU test using Consel v.1.20 (Shimodaira and Hasegawa  
301 2001). In order to detect possible introgression among species of each quartet, first we estimated  
302 a species network with PhyloNet using a full maximum likelihood approach (Yu et al. 2014)  
303 with 100 runs per search while optimizing the likelihood of the branch lengths and inheritance  
304 probabilities for every proposed species network. Furthermore, we also carried out the  
305 ABBA/BABA test to detect introgression (Green et al. 2010; Durand et al. 2011) in each of four-  
306 taxon species trees. We calculated the  $D$ -statistic and associated  $z$  score for the null hypothesis of  
307 no introgression ( $D = 0$ ) following each quartet ASTRAL species tree for taxon order assignment  
308 using 100 jackknife replicates and a block size of 10,000 bp with evobiR v1.2 (Blackmon and  
309 Adams) in R.

310         Additionally, to detect any non-random genomic block of particular quartet topology  
311 (Fontaine et al. 2015), we mapped the physical location of genes supporting each alternative

312 quartet topology onto the *Beta vulgaris* reference genome using a synteny approach (See  
313 Supplemental Information for details).

314

315 *Assessment of substitutional saturation, codon usage bias, compositional heterogeneity, and*  
316 *model of sequence evolution misspecification*

317 Analyses were carried out in a 11-taxon dataset [referred herein as 11-taxon(tree); Fig. S1] that  
318 included the same taxa used for species network analyses, but was processed differently to  
319 account for codon structure (see Supplemental Methods for details). Saturation was evaluated by  
320 plotting the uncorrected genetic distances of the concatenated alignment against the inferred  
321 distances (see Supplemental Methods for details). To determine the effect of saturation in the  
322 phylogenetic inferences we estimated individual ML gene trees using an unpartitioned  
323 alignment, a partition by first and second codon positions, and the third codon positions, and by  
324 removing all third codon positions. All tree searches were carried out in RAxML with a  
325 GTRGAMMA model and 200 bootstrap replicates. We then estimated a coalescent-based species  
326 tree and explored gene tree discordance with PhyParts.

327 Codon usage bias was evaluated using a correspondence analysis of the Relative  
328 Synonymous Codon Usage (RSCU; see Supplemental Methods for details). To determine the  
329 effect of codon usage bias in the phylogenetic inferences we estimated individual gene trees  
330 using codon-degenerated alignments (see Supplemental Methods for details). Gene tree inference  
331 and discordance analyses were carried out on the same three data schemes as previously  
332 described.

333 Among-lineage compositional heterogeneity was evaluated on individual genes using a  
334 compositional homogeneity test (Supplemental Methods for details). To assess if compositional

335 heterogeneity had an effect in species tree inference and gene tree discordance, gene trees that  
336 showed the signal of compositional heterogeneity were removed from saturation and codon  
337 usage analyses and the species tree and discordance analyses were rerun.

338 To explore the effect of sequence evolution model misspecification, we reanalyzed the  
339 datasets from the saturation and codon usage analyses using inferred gene trees that accounted  
340 for model selection. Additionally, we also explored saturation and model misspecification in  
341 phylogenetic trees from amino acid alignments (see Supplemental Methods for details).

342

#### 343 *Polytomy test*

344 To test if the gene tree discordance among the main clades of Amaranthaceae s.l. could be  
345 explained by polytomies instead of bifurcating nodes, we carried out the quartet-based polytomy  
346 test by Sayyari and Mirarab (2018) as implemented in ASTRAL. We performed the polytomy  
347 test using the gene trees inferred from the saturation and codon usage analyses [11-taxon(tree)  
348 dataset]. Because this test can be sensitive to gene tree error (Sayyari and Mirarab 2018), we  
349 performed a second test using gene trees where branches with less than 75% of bootstrap support  
350 were collapsed.

351

#### 352 *Coalescent simulations*

353 To investigate if gene tree discordance can be explained by ILS alone, we carried out coalescent  
354 simulations similar to Cloutier et al. (2019). An ultrametric species tree with branch lengths in  
355 mutational units ( $\mu T$ ) was estimated by constraining an ML tree search of the 11-taxon(net)  
356 concatenated alignment to the ASTRAL species tree topology with a GTR+GAMMA model  
357 while enforcing a strict molecular clock in PAUP v4.0a (build 165; Swofford 2002). The



358 mutational branch lengths from the constrained tree and branch lengths in coalescent units ( $\tau =$   
359  $T/4N_e$ ) from the ASTRAL species trees were used to estimate the population size parameter  $\theta$   
360 ( $\theta = \mu T/\tau$ ; Degnan and Rosenberg 2009) for internal branches. Terminal branches were set with a  
361 population size parameter  $\theta$  of one. We used the R package Phybase v. 1.4 (Liu and Yu 2010)  
362 that uses the formula from Rannala and Yang (2003) to simulate 10,000 gene trees using the  
363 constraint tree and the estimated  $\theta$  values. Then we calculated the distribution of Robinson  
364 and Foulds (1981) tree-to-tree distances between the species tree and each gene tree using the R  
365 package Phangorn v2.5.3 (Schliep 2011), and compared this with the distribution of tree-to-tree  
366 distances between the species tree and the simulated gene tree. We ran simulations using the  
367 species tree and associated gene tree distribution from the original no partition 11-taxon(net).

368

#### 369 *Test of the anomaly zone*

370 The anomaly zone occurs where a set of short internal branches in the species tree produces gene  
371 trees that differ from the species tree more frequently than those that are concordant [ $a(x)$ ; as  
372 defined in equation 4 of Degnan and Rosenberg (2006)]. To explore if gene tree discordance  
373 observed in Amaranthaceae s.l. is a product of the anomaly zone, we estimated the boundaries of  
374 the anomaly zone [ $a(x)$ ; as defined in equation 4 of Degnan and Rosenberg (2006)] for the  
375 internal nodes of the species tree. Here,  $x$  is the branch length in coalescent units in the species  
376 tree that has a descendant internal branch. If the length of the descendant internal branch ( $y$ ) is  
377 smaller than  $a(x)$ , then the internode pair is in the anomaly zone and is likely to produce  
378 anomalous gene trees (AGTs). We carried out the calculation of  $a(x)$  following Linkem et al.  
379 (2016) in the same 11-taxon(tree) ASTRAL species tree used for coalescent simulations.  
380 Additionally, to establish the frequency of gene trees that were concordant with the estimated

381 species trees, we quantified the frequency of all 105 possible rooted gene trees with  
382 Amaranthaceae s.l. being monophyletic.

383

## 384 RESULTS

### 385 *Transcriptome sequencing, assembly, translation, and quality control*

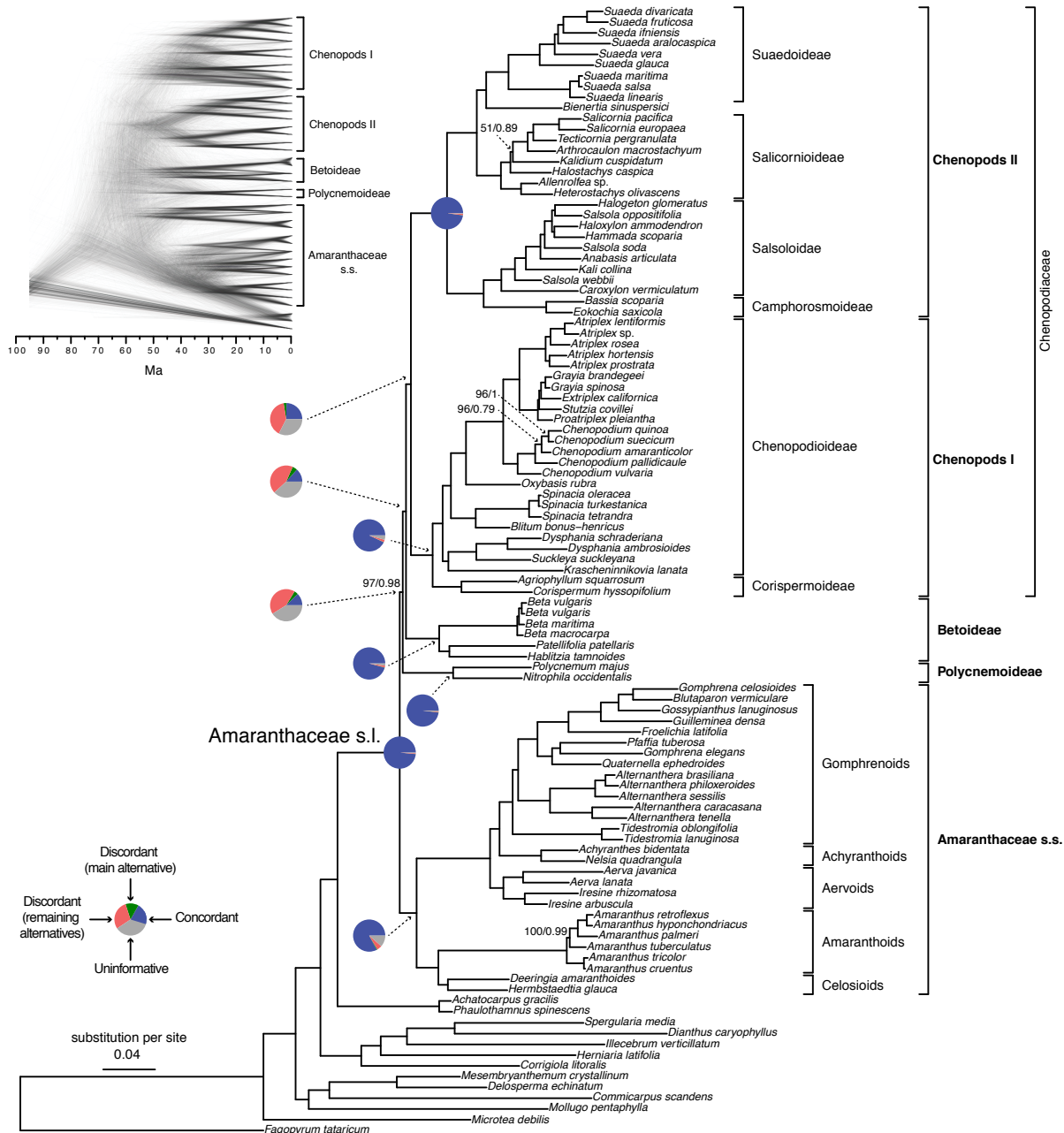
386 Raw reads for the 17 newly generated transcriptomes are available from the NCBI Sequence  
387 Read Archive (BioProject: PRJNA640363; Table S2). The number of raw read pairs ranged from  
388 17 to 27 million. For the 16 samples processed using RiboZero, organelle reads accounted for  
389 15% to 52% of read pairs (Table S2). For *Tidestromia oblongifolia* that poly-A enrichment was  
390 carried out in library prep with ~5% of raw reads were from organelle (Table S2). The final  
391 number of orthologs was 13,024 with a mean of 9,813 orthologs per species (Table S1). Of  
392 those, 82 orthologs had a strong signal of recombination ( $P \leq 0.05$ ) and were removed from  
393 downstream analyses.

394

### 395 *Analysis of the nuclear dataset of Amaranthaceae s.l.*

396 The final set of nuclear orthologous genes included 936 genes with at least 99 out of 105 taxa  
397 and 1,000 bp in aligned length after removal of low occupancy columns (the 105-taxon dataset).  
398 The concatenated matrix consisted of 1,712,054 columns with a gene and character occupancy of  
399 96% and 82%, respectively. The species tree from ASTRAL and the concatenated ML tree from  
400 RAxML recovered the exact same topology with most clades having maximal support [i.e.,  
401 bootstrap percentage (BS) = 100, local posterior probabilities (LPP) = 1; Fig. 2; Figs S2–S3].  
402 Both analyses recovered Chenopodiaceae as monophyletic with the relationships among major  
403 clades concordant with the cpDNA analysis from Kadereit et al. (2017; Fig. 1d). Betoideae was

404 placed as sister of Chenopodiaceae, while Polycnemoideae was strongly supported as sister (BS  
 405 = 97, LPP = 0.98) to the clade composed of Chenopodiaceae and Betoideae. Amaranthaceae s.s.  
 406 had an overall topology concordant to Kadereit et al. (2017), with the exception of *Iresine*, which  
 407 was recovered among the Aervoids (Fig. 2; Figs S2–S3).  
 408



410 **FIGURE 2.** Maximum likelihood phylogeny of Amaranthaceae s.l. inferred from RAxML  
411 analysis of the concatenated 936-nuclear gene supermatrix, which had the same topology as  
412 recovered from ASTRAL. All nodes have maximal support (bootstrap = 100/ASTRAL local  
413 posterior probability = 1) unless noted. Pie charts present the proportion of gene trees that  
414 support that clade (blue), support the main alternative bifurcation (green), support the remaining  
415 alternatives (red), and the proportion (conflict or support) that have < 50% bootstrap support  
416 (gray). Only pie charts for major clades are shown (see Fig. S2 for all node pie charts). Branch  
417 lengths are in number of substitutions per site. The inset (top left) shows the Densitree  
418 cloudogram inferred from 1,242 nuclear genes for the reduced 41-taxon dataset.  
419

420         The conflict analyses confirmed the monophyly of Amaranthaceae s.l. with 922 out of  
421 930 informative gene trees being concordant (ICA= 0.94) and having full QS support (1/–/1; i.e.,  
422 all sampled quartets supported that branch). Similarly, the monophyly of Amaranthaceae s.s. was  
423 highly supported by 755 of 809 informative gene trees (ICA =0.85) and the QS scores (0.92/0/1).  
424 However, the backbone of the family was characterized by high levels of gene tree discordance  
425 (Fig. 2; Figs S2–S3). The monophyly of Chenopodiaceae was supported only by 231 out of 632  
426 informative gene trees (ICA = 0.42) and the QS score (0.25/0.19/0.99) suggested weak quartet  
427 support with a skewed frequency for an alternative placement of two well-defined clades within  
428 Chenopodiaceae, herein referred to as ‘Chenopods I’ and ‘Chenopods II’ (Fig. 2; Figs S2–S3).  
429 ‘Chenopods I’ and ‘Chenopods II’ were each supported by the majority of gene trees, 870 (ICA  
430 = 0.89) and 916 (ICA = 0.91), respectively and full QS support. Similarly, high levels of conflict  
431 among informative gene trees were detected in the placement of Betoideae (126 out of 579  
432 informative genes being concordant, ICA = 0.28; QS score 0.31/0.57/1) and Polycnemoideae  
433 (116/511; ICA = 0.29;0.3/0.81/0.99). The Densitree cloudogram also showed significant conflict  
434 along the backbone of Amaranthaceae s.l. (Fig. 2).

435 Together, analysis of nuclear genes recovered five well-supported clades in  
436 Amaranthaceae s.l.: Amaranthaceae s.s., Betoideae, ‘Chenopods I’, ‘Chenopods II’, and  
437 Polycnemoideae. However, relationships among these five clades showed a high level of conflict  
438 among genes [ICA scores and gene counts (pie charts)] and among subsampled quartets (QS  
439 scores), despite having high support from both BS and LPP scores.

440

441 *Plastid phylogenetic analysis of Amaranthaceae s.l.*

442 RNA editing prediction analysis revealed editing sites only on CDS sequences of  
443 reference plastomes (Table S3), suggesting that cpDNA reads in RNA-seq libraries come from  
444 RNA rather than DNA leftover from incomplete DNase digestion during sample processing (See  
445 Discussion for details in plastid assembly from RNA-seq data).

446 The final alignment from 76 genes included 103 taxa and 55,517 bp in aligned length.  
447 The ML tree recovered the same five main clades within Amaranthaceae s.l. with maximal  
448 support (BS = 100; Figs S4–S6). Within each main clade, relationships were fully congruent  
449 with Kadereit et al. (2017) and mostly congruent with our nuclear analyses. However, the  
450 relationship among the five main clades differed from the nuclear tree. Here, the sister  
451 relationships between Betoideae and ‘Chenopods I’, and between Amaranthaceae s.s. and  
452 Polycnemoideae were both supported by BS = 100. The sister relationship between these two  
453 larger clades was moderately supported (BS = 73), leaving ‘Chenopods II’ as sister to the rest of  
454 Amaranthaceae s.l.

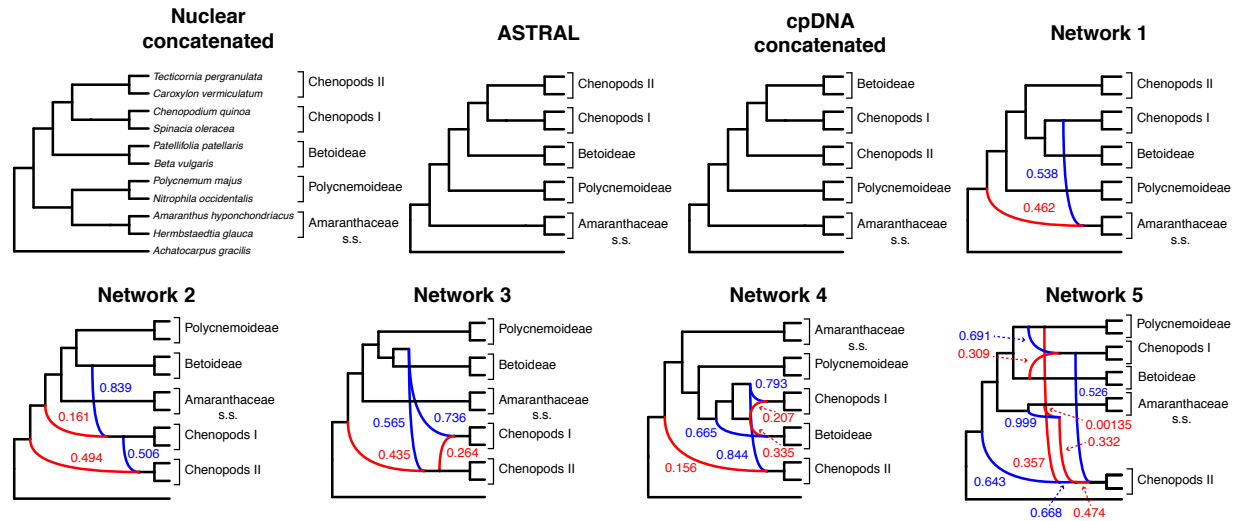
455 Conflict analysis confirmed the monophyly of Amaranthaceae s.l. with 51 out of 69  
456 informative gene trees supporting this clade (ICA = 0.29) and full QS support (1/–/1). On the  
457 other hand, and similar to the nuclear phylogeny, significant gene tree discordance was detected

458 among plastid genes regarding placement of the five major clades (Figs S4–S6). The sister  
459 relationship of Betoideae and 'Chenopods I' was supported by only 20 gene trees (ICA = 0.06),  
460 but it had a strong support from QS (0.84/0.88/0/94). The relationship between Amaranthaceae  
461 s.s. and Polycnemoideae was supported by only 15 gene trees (ICA = 0.07), while QS showed  
462 weak support (0.41/0.21/0.78) with signals of a supported secondary evolutionary history. The  
463 clade uniting Betoideae, 'Chenopods I', Amaranthaceae s.s., and Polycnemoideae was supported  
464 by only four-gene trees, with counter-support from both QS (-0.29/0.42/0.75) and ICA (-0.03),  
465 suggesting that most gene trees and sampled quartets supported alternative topologies.

466

467 *Species network analysis of Amaranthaceae s.l.*

468 The reduced 11-taxon(net) dataset included 4,138 orthologous gene alignments with no missing  
469 taxon and a minimum of 1,000 bp (aligned length after removal of low occupancy columns). The  
470 11-taxon(net) ASTRAL species tree was congruent with the 105-taxon tree, while both the  
471 nuclear and plastid ML trees from concatenated supermatrices had different topologies than their  
472 corresponding 105-taxon trees (Fig. 3). Model selection indicated that any species network was a  
473 better model than the best bifurcating nuclear or plastid trees (ASTRAL; AICc = 46972.9794;  
474 Table S5). PhyloNet identified up to five hybridization events among the clades of  
475 Amaranthaceae s.l. (Fig. 3), with the best model having five hybridization events involving all  
476 five clades (AICc = 28459.1835; Table S5). The best species network did not support the  
477 hypothesis of the hybrid origin of Betoideae or Polycnemoideae. Moreover, the best species  
478 network showed a complex reticulate pattern that involved mainly 'Chenopods I' and  
479 'Chenopods II' (Fig. 3), but none of these reticulations events were supported by *D*-Statistic or  
480 species network results from the four-taxon analyses (see below).



481

482 **FIGURE 3.** Species trees and species networks of the reduced 11-taxon(net) dataset of  
483 Amaranthaceae s.l. Nuclear concatenated phylogeny inferred from 4,138-nuclear gene  
484 supermatrix with RAxML. ASTRAL species tree inferred using 4,138 nuclear genes. cpDNA  
485 concatenated tree inferred from 76-plastid gene supermatrix with IQ-tree. Species network  
486 inferred from PhyloNet pseudolikelihood analyses with 1 to 5 maximum number of reticulations.  
487 Red and blue indicate the minor and major edges, respectively, of hybrid nodes. Number next to  
488 the branches indicates inheritance probabilities for each hybrid node.

489

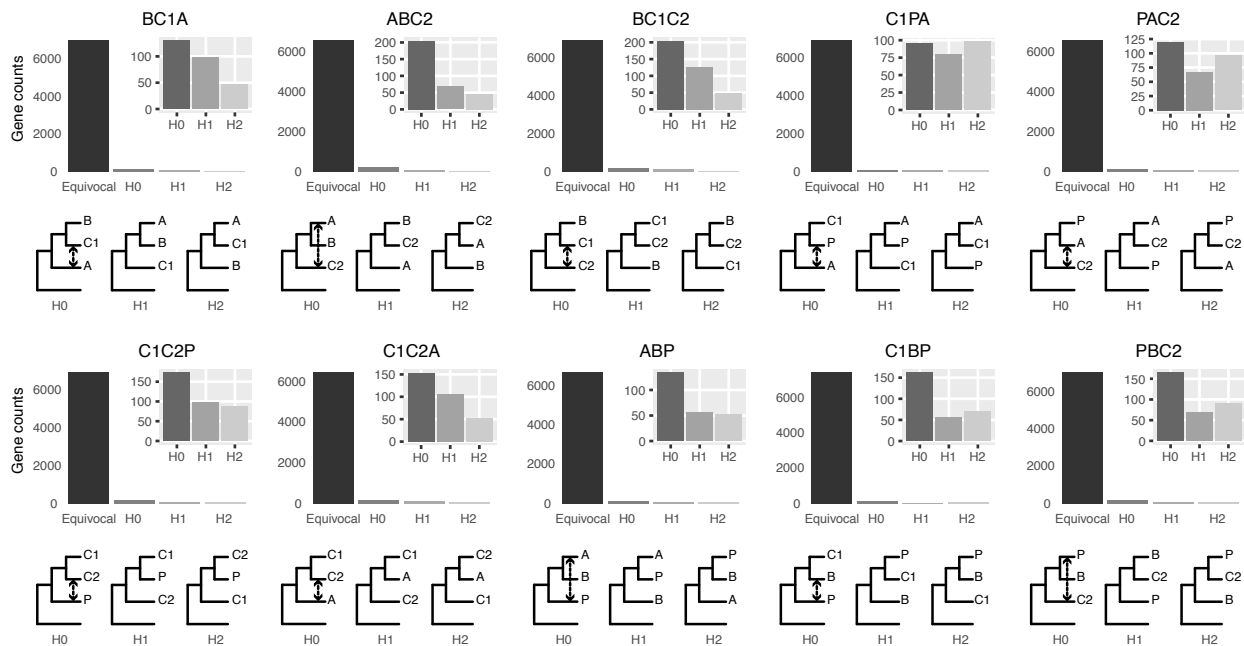
490

#### *Four-taxon analyses*

491 To test for hybridization events one at a time, we further reduced the 11-taxon(net) dataset to 10  
492 four-taxon combinations that each included one outgroup and one representative each from three  
493 out of the five major ingroup clades. Between 7,756 and 8,793 genes were used for each quartet  
494 analysis (Table S6) and each quartet topology can be found in Figure 4. Only five out of the ten  
495 bifurcating quartet species trees (H0 and more frequent gene tree) were compatible with the  
496 nuclear species tree inferred from the complete 105-taxon dataset. The remaining quartets  
497 corresponded to the second most frequent gene tree topology in the 105-taxon nuclear tree,

498 except for the quartet of Betoideae, ‘Chenopods II’ and Polycnemoideae (PBC2, which  
 499 correspond to the least frequent gene tree).

500



501

502 **FIGURE 4.** Gene counts from Approximate-Unbiased (AU) topology test of the 10 quartets from  
 503 the five main clades of Amaranthaceae s.l. AU tests were carried out between the three possible  
 504 topologies of each quartet. H0 represents the ASTRAL species tree of each quartet. “Equivocal”  
 505 indicates gene trees that fail to reject all three alternative topologies for a quartet with  $p \leq 0.05$ .  
 506 Gene counts for each of the three alternative topologies represent gene trees supporting  
 507 unequivocally one topology by rejecting the other two alternatives with  $p \leq 0.05$ . Insets represent  
 508 gene counts only for unequivocal topology support. Double arrowed lines in each H0 quartet  
 509 represent the direction of introgression from the ABBA/BABA test. Each quartet is named  
 510 following the species tree topology, where the first two species are sister to each other. A =  
 511 Amaranthaceae s.s. (represented by *Amaranthus hypochondriacus*), B = Betoideae (*Beta*  
 512 *vulgaris*), C1 = Chenopods I (*Chenopodium quinoa*), C2 = Chenopods II (*Caroxylum*  
 513 *vermiculatum*), P = Polycnemoideae (*Polycnemonum majus*). All quartets are rooted with  
 514 *Mesembryanthemum crystallinum*.

515



516 In each of the ten quartets, the ASTRAL species tree topology (H0) was the most  
517 frequent among individual gene trees (raw counts) but only accounted for 35%–41% of gene  
518 trees, with the other two alternative topologies having balanced to slightly skewed frequencies  
519 (Fig. S7a; Table S7). Gene counts based on the raw likelihood scores from the constraint  
520 analyses showed similar patterns (Fig. S7b; Table S7). When filtered by significant likelihood  
521 support (i.e.,  $\Delta\text{AICc} \geq 2$ ), the number of trees supporting each of the three possible topologies  
522 dropped between 34% and 45%, but the species tree remained the most frequent topology for all  
523 quartets (Fig. S7b; Table S7). The AU topology tests failed to reject ( $P \leq 0.05$ ) approximately  
524 85% of the gene trees for any of the three possible quartet topologies and rejected all but a single  
525 topology in only 3%–4.5% of cases. Among the unequivocally selected gene trees, the  
526 frequencies among the three alternative topologies were similar to ones based on raw likelihood  
527 scores (Fig S7; Table S7). Therefore, topology tests showed that most genes were uninformative  
528 for resolving the relationships among the major groups of Amaranthaceae s.l.

529 Across all ten quartets we found that most genes had very low TC scores (for any single  
530 node the maximum TC value is 1; Supplemental Fig. S8), showing that individual gene trees also  
531 had high levels of conflict among bootstrap replicates, which also indicated uninformative genes  
532 and was concordant with the AU topology test results. We were unable to detect any significant  
533 correlation between TC scores and alignment length, GC content or alignment gap fraction  
534 (Table S8), suggesting that filtering genes by any of these criteria was unlikely to increase the  
535 information content of the dataset.

536 Species network analyses followed by model selection using each of the four-taxon  
537 datasets showed that in seven out of the ten total quartets, the network with one hybridization  
538 event was a better model than any bifurcating tree topology. However, each of the best three

539 networks from PhyloNet had very close likelihood scores and no significant  $\Delta\text{AICc}$  among them  
540 (Table S6; Fig S9). For the remaining three quartets, the species trees (H0) was the best model.

541 The ABBA/BABA test results showed a significant signal of introgression within each of  
542 the ten quartets (Table S9; Fig 4). The possible introgression was detected between six out of the  
543 ten possible pairs of taxa. Potential introgression between Betoideae and Amaranthaceae s.s.,  
544 ‘Chenopods I’ or ‘Chenopods II’, and between ‘Chenopods I’ and Polycnemoideae was not  
545 detected.

546 To further evaluate whether alternative quartets were randomly distributed across the  
547 genome, we mapped topologies from the quartet of Betoideae, ‘Chenopods II, and  
548 Amaranthaceae s.s. (BC1A) onto the reference genome of *Beta vulgaris*. We used the BC1A  
549 quartet as an example as all four species in this quartet have reference genomes. Synteny analysis  
550 between the diploid ingroup reference genome *Beta vulgaris* and the diploid outgroup reference  
551 genome *Mesembryanthemum crystallinum* recovered 22,179 collinear genes in 516 syntenic  
552 blocks. With the collinear ortholog pair information, we found that of the 8,258 orthologs of the  
553 BC1A quartet, 6,941 contained syntenic orthologous genes within 383 syntenic blocks. The  
554 distribution of the BC1A quartet topologies along the chromosomes of *Beta vulgaris* did not  
555 reveal any spatial clustering of any particular topology along the chromosomes (Fig. S10).

556 Gene Ontology enrichment analyses (not shown) using alternative topologies of the  
557 BC1A quartet did not recover any significant term associated with C<sub>4</sub> photosynthesis, drought  
558 recovery, or salt stress response.

559

560

561 *Assessment of substitutional saturation, codon usage bias, compositional heterogeneity,*  
562 *sequence evolution model misspecification, and polytomy test.*

563 We assembled a second 11-taxon(tree) dataset that included 5,936 genes and a minimum of 300  
564 bp (aligned length after removal of low occupancy columns) and no missing taxon. The  
565 saturation plots of uncorrected and predicted genetic distances showed that the first and second  
566 codon positions were unsaturated ( $y = 0.884x$ ), whereas the slope of the third codon positions ( $y$   
567  $= 0.571x$ ) showed a signal of saturation (Fig. S11). The correspondence analyses of RSCU show  
568 that some codons are more frequently used in different species, but overall the codon usage was  
569 randomly dispersed among all species and not clustered by clade (Fig. S12). This suggests that  
570 the phylogenetic signal is unlikely to be driven by differences in codon usage bias among clades.  
571 Furthermore, only 549 (~9%) genes showed a signal of compositional heterogeneity ( $p < 0.05$ ).  
572 The topology and support (LPP = 1.0) for all branches was the same for the ASTRAL species  
573 trees obtained from the different data schemes while accounting for saturation, codon usage,  
574 compositional heterogeneity, and model of sequence evolution, and was also congruent with the  
575 ASTRAL species tree and concatenated ML from the 105-taxon analyses (Fig. S13). In general,  
576 the proportion of gene trees supporting each bipartition remained the same in every analysis and  
577 showed high levels of conflict among the five major clades of Amaranthaceae s.l. (Fig S13).

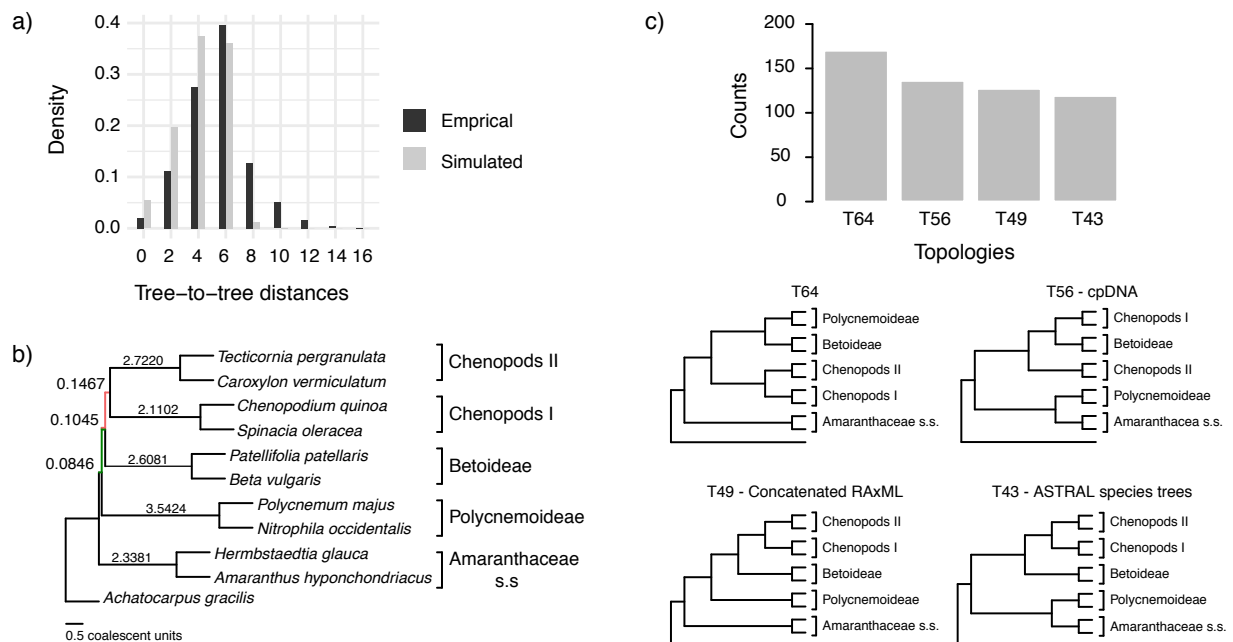
578 The ASTRAL polytomy test resulted in the same bifurcating species tree for the 11-  
579 taxon(tree) dataset and rejected the null hypothesis that any branch is a polytomy ( $p < 0.01$  in all  
580 cases). These results were identical when using gene trees with collapsed branches.

581

582  
583  
584  
585  
586  
587  
588  
589  
590  
591  
592  
593

*Coalescent simulations and tests of the anomaly zone*

The distribution of tree-to-tree distances of the empirical and simulated gene trees to the species tree from the 11-taxon(tree) dataset largely overlapped (Fig 5a), suggesting that ILS alone is able to explain most of the observed gene tree heterogeneity (Maureira-Butler et al. 2008). The anomaly zone limit calculations using species trees from the 11-taxon(tree) dataset detected two pairs of internodes among the five major groups in Amaranthaceae s.l. that fell into the anomaly zone (the red pair and the green pair, Fig. 5b; Table S10). Furthermore, gene tree counts showed that the species tree was not the most common gene tree topology, as defined for the anomaly zone (Degnan and Rosenberg 2006; Fig 5c). The species tree was the fourth most common gene tree topology (119 out of 4,425 gene trees), while the three most common gene tree topologies occurred 170, 136, and 127 times (Fig. 5c).



594  
595  
596

**FIGURE 5.** Coalescent simulations and tests of the anomaly zone from the 11-taxon(tree) dataset estimated from individual gene trees. a) Distribution of tree-to-tree distances between empirical

597 gene trees and the ASTRAL species tree, compared to those from the coalescent simulation. b)  
598 ASTRAL species tree showing branch length in coalescent units. Green and red branches  
599 represent the internodes that fall in the anomaly zone (see Table S10 for anomaly zone limits). c)  
600 Gene tree counts (top) of the four most common topologies (bottom). Gene trees that do not  
601 support the monophyly of any of the five major clades were ignored.

602

603

## DISCUSSION

604 The exploration of gene tree discordance has become a fundamental step to understand  
605 recalcitrant relationships across the Tree of Life. Recently, new tools have been developed to  
606 identify and visualize gene tree discordance (e.g., Salichos et al. 2014; Smith et al. 2015; Huang  
607 et al. 2016; Pease et al. 2018). However, downstream methods that evaluate processes generating  
608 observed patterns of gene tree discordance are still in their infancy. In this study, by combining  
609 transcriptomes and genomes, we were able to create a rich and dense dataset to start to tease  
610 apart alternative hypotheses concerning the sources of conflict along the backbone phylogeny of  
611 Amaranthaceae s.l. We found that gene tree heterogeneity observed in Amaranthaceae s.l. can be  
612 explained by a combination of processes, including ILS, ancient hybridization, and  
613 uninformative genes, that might have acted simultaneously and/or cumulatively.

614

615

### *Gene tree discordance detected among plastid genes*

616 Although both our concatenation-based plastid and nuclear phylogenies supported the same five  
617 major clades of Amaranthaceae s.l., the relationships among these clades are incongruent (Figs. 2  
618 & S4). Cytonuclear discordance is well-known in plants and it has been traditionally attributed to  
619 reticulate evolution (Rieseberg and Soltis 1991; Sang et al. 1995; Soltis and Kuzoff 1995). Such  
620 discordance continues to be treated as evidence in support of hybridization in more recent  
621 phylogenomic studies that assume the plastome to be a single, linked locus (e.g., Folk et al.

622 2017; Vargas et al. 2017; Morales-Briones et al. 2018b; Lee-Yaw et al. 2019). However, recent  
623 work showed that the plastome might not necessarily act as a single locus and high levels of tree  
624 conflict have been detected (Gonçalves et al. 2019; Walker et al. 2019).

625 In Amaranthaceae s.l., previous studies based on plastid protein-coding genes or introns  
626 (Fig. 1; Kadereit et al. 2003; Müller and Borsch 2005; Hohmann et al. 2006; Kadereit et al.  
627 2017) resulted in different relationships among the five main clades and none in agreement with  
628 our 76-gene plastid phylogeny. Our conflict and QS analyses of the plastid dataset (Figs S5–S6)  
629 revealed strong signals of gene tree discordance among the five major clades of Amaranthaceae  
630 s.l., likely due to heteroplasmy, although the exact sources of conflict are yet to be clarified  
631 (Gonçalves et al. 2019). Unlike the results found by Walker et al. (2019), our individual plastid  
632 gene trees had highly supported nodes (i.e.,  $BS \geq 70$ , Fig S5), suggesting that low phylogenetic  
633 information content is not the main source of conflict in our plastid dataset.

634 Our results support previous studies showing RNA-seq data can be a reliable source for  
635 plastome assembly (Smith 2013; Osuna-Mascaró et al. 2018; Gitzendanner et al. 2018). RNA-  
636 seq libraries can contain some genomic DNA due to incomplete digestion during RNA  
637 purification (Smith 2013). Given the AT-rich nature of plastomes, plastid DNA may survive the  
638 poly-A selection during mRNA enrichment (Schliesky et al. 2012). However, RNA editing  
639 prediction results showed that our Amaranthaceae s.l. cpDNA assemblies came from RNA rather  
640 than DNA contamination regardless of library preparation by poly-A enrichment (71  
641 transcriptomes) or RiboZero (16 transcriptomes). Similarly, Osuna-Mascaró et al. (2018) also  
642 found highly similar plastome assemblies (i.e., general genome structure, and gene number and  
643 composition) from RNA-seq and genomic libraries, supporting the idea that plastomes are fully  
644 transcribed in photosynthetic eukaryotes (Shi et al. 2016). Furthermore, the backbone topology

645 of our plastid tree built mainly from RNA-seq data (97 out of 105 samples) was consistent with a  
646 recent complete plastome phylogeny of Caryophyllales mainly from genomic DNA (Yao et al.  
647 2019), showing the utility of recovering plastid gene sequences from RNA-seq data.  
648 Nonetheless, RNA editing might be problematic when combining samples from RNA-seq and  
649 genomic DNA, especially when resolving phylogenetic relationships among closely related  
650 species.

651

652 *Identifiability in methods for detecting reticulation events*

653 All methods that we used to detect ancient hybridization inferred the presence of reticulation  
654 events. However, our results suggest that these methods all struggle with ancient, rapid  
655 radiations. Advances have been made in recent years in developing methods to infer species  
656 networks in the presence of ILS (reviewed in Elworth et al. 2019). These methods have been  
657 increasingly used in phylogenetic studies (e.g., Wen et al. 2016; Copetti et al. 2017; Morales-  
658 Briones et al. 2018a; Crowl et al. 2020). To date, however, species network inference is still  
659 computationally intensive and limited to a small number of species and a few hybridization  
660 events (Hejase and Liu 2016; but see Hejase et al. 2018 and Zhu et al. 2019). Furthermore,  
661 studies evaluating the performance of different phylogenetic network inference approaches are  
662 scarce and restricted to simple hybridization scenarios. Kamneva and Rosenberg (2017) showed  
663 that likelihood methods like Yu et al. (2014) are often robust to ILS and gene tree error when  
664 symmetric hybridization (equal genetic contribution of both parents) events are considered.  
665 While this approach usually does not overestimate hybridization events, it fails to detect skewed  
666 hybridization (unequal genetic contribution of both parents) events in the presence of significant  
667 ILS. Methods developed to scale to larger numbers of species and hybridizations like the ones

668 using pseudo-likelihood approximations (i.e., Solís-Lemus and Ané 2016; Yu and Nakhleh 2015)  
669 are yet to be evaluated independently, but in the case of the Yu and Nakhleh (2015) method  
670 based on rooted triples, it cannot distinguish the correct network when other networks can  
671 produce the same set of triples (Yu and Nakhleh 2015). On the other hand, the method of Solís-  
672 Lemus and Ané (2016), based on unrooted quartets, is better at avoiding indistinguishable  
673 networks, but it is limited to only level-1 network scenarios.

674         Applying the above methods to our data set recovered multiple reticulation events.  
675 Analysis of our 11-taxon(net) dataset using a pseudo-likelihood approach detected up to five  
676 hybridization events involving all five major clades of Amaranthaceae s.l. (Fig. 3). Model  
677 selection, after calculating the full likelihood of the obtained networks, also chose the 5-  
678 reticulation species as the best model. Likewise, we found that any species network had a better  
679 ML score than a bifurcating tree (Table S5). However, further analyses demonstrated that full  
680 likelihood network searches with up to one hybridization event are indistinguishable from each  
681 other (Table S6), resembling a random gene tree distribution. This pattern can probably be  
682 explained by the high levels of gene tree discordance and lack of phylogenetic signal in the  
683 inferred quartet gene trees (Fig. 4), suggesting that the 11-taxon(net) network searches can  
684 potentially overestimate reticulation events due to high levels of gene tree error or ILS.

685         Using the *D*-Statistic (Green et al. 2010; Durand et al. 2011) we also detected signals of  
686 introgression in seven possible locations among the five main groups of Amaranthaceae s.l.  
687 (Table S9). The inferred introgression events agreed with at least one of the reticulation  
688 scenarios from the phylogenetic network analysis. However, the *D*-Statistic did not detect any  
689 introgression that involves Betoideae, which was detected in the phylogenetic network analysis  
690 with either four or five reticulations events. The *D*-Statistic has been shown to be robust to a



691 wide range of divergence times, but it is sensitive to relative population size (Zheng and Janke  
692 2018), which agrees with the notion that large effective population sizes and short branches  
693 increase the chances of ILS (Pamilo and Nei 1988) and in turn can dilute the signal for the *D*-  
694 Statistic (Zheng and Janke 2018). Recently, Elworth et al. (2018) found that multiple or ‘hidden’  
695 reticulations can cause the signal of the *D*-statistic to be lost or distorted. Furthermore, when  
696 multiple reticulations are present, the traditional approach of dividing datasets into quartets can  
697 be problematic as it largely underestimates *D* values (Elworth et al. 2018). Given short internal  
698 branches in the backbone of Amaranthaceae s.l. and the phylogenetic network results showing  
699 multiple hybridizations, it is plausible that our *D*-statistic may be affected by these issues.

700 Our analysis highlights problems with identifiability in relying on *D*-statistic or  
701 phylogenetic network analysis alone to detect reticulation events, especially in cases of ancient  
702 and rapid diversification. Both analyses resulted in highly complex and inconsistent reticulate  
703 scenarios that cannot be distinguished from ILS or gene tree error. Hence, despite the use of  
704 genome-scale data and exhaustive hypothesis testing, support is lacking for the hybrid origin of  
705 Polcnemoideae or Betoideae, or any particular hybridization event among major groups in  
706 Amaranthaceae s.l. In addition to potential hybridization events, rapid speciation, short branches,  
707 and large ancestral population size all impacting our ability to resolve relationships among major  
708 clades in Amaranthaceae s.l. Simulating combinations of these scenarios is beyond the scope of  
709 this particular manuscript.

710

### 711 *ILS and the Anomaly Zone*

712 ILS is ubiquitous in multi-locus phylogenetic datasets. In its most severe cases ILS produces the  
713 ‘anomaly zone’, defined as a set of short internal branches in the species tree that produce

714 anomalous gene trees (AGTs) that are more likely than the gene tree that matches the species tree  
715 (Degnan and Rosenberg 2006). Rosenberg (2013) expanded the definition of the anomaly zone  
716 to require that a species tree contain two consecutive internal branches in an ancestor–descendant  
717 relationship in order to produce AGTs. To date, only a few empirical examples of the anomaly  
718 zone have been reported (Linkem et al. 2016; Cloutier et al. 2019). Our results show that the  
719 species tree of Amaranthaceae s.l. has three consecutive short internal branches that lay within  
720 the limits of the anomaly zone (i.e.,  $y < a[x]$ ; Fig. 5; Table S10) and that the species tree is not  
721 the most frequent gene tree (Fig. 4). While both lines of evidence support the presence of AGTs,  
722 it is important to point out that our quartet analysis showed that most quartet gene trees were  
723 equivocal (94–96%; Fig. 4), and therefore, were uninformative. Huang and Knowles (2009)  
724 pointed out that the gene tree discordance produced from the anomaly zone can be produced by  
725 uninformative gene trees and that for species trees with short branches the most probable gene  
726 tree topology is a polytomy rather than an AGT. Our ASTRAL polytomy test, however, rejected  
727 a polytomy along the backbone of Amaranthaceae s.l. in any of the gene tree sets used. While we  
728 did not test for polytomies in individual gene trees, our ASTRAL polytomy test using gene trees  
729 with branches of <75% bootstrap support collapsed also rejected the presence of a polytomy.  
730 Therefore, the distribution of gene tree frequency in combination with short internal branches in  
731 the species tree supports the presence of an anomaly zone in Amaranthaceae s.l.

732

733

#### *Taxonomic implications*

734 Despite the strong signal of gene tree discordance, both nuclear and plastid datasets strongly  
735 supported five major clades within Amaranthaceae s.l.: Amaranthaceae s.s, ‘Chenopods I’,  
736 ‘Chenopods II’, Betoideae, and Polycnemoideae (Figs. 2 & S4). These five clades are congruent

737 with morphology and previous taxonomic treatments of the group. However, the relationships  
738 among these five lineages remain elusive with our data. Taken together, our tests of sources of  
739 incongruence for these early-diverging nodes indicate that no single source such as a particular  
740 ancient hybridization event can confidently account for the strong signal of gene tree  
741 discordance, suggesting that the discordance results primarily from ancient and rapid lineage  
742 diversification. Thus, the backbone of Amaranthaceae s.l. remains, and likely will remain,  
743 unresolved even with genome-scale data. The stem age of Amaranthaceae s.l. dates back to the  
744 early Tertiary (Paleocene; Kadereit et al. 2012; Di Vincenzo et al. 2018; Yao et al. 2019), but  
745 due to nuclear and plastid gene tree along the backbone, the geographic origin of Amaranthaceae  
746 s.l. remains ambiguous.

747 Therefore, for the sake of taxonomic stability, we suggest retaining Amaranthaceae s.l.  
748 sensu APG IV (The Angiosperm Phylogeny Group 2016), which includes the previously  
749 recognized Chenopodiaceae. Amaranthaceae s.l. is characterized by a long list of anatomical,  
750 morphological and phytochemical characters such as minute sessile flowers with five tepals, a  
751 single whorl of epitepalous stamens, and one basal ovule (Kadereit et al. 2003). Here, we  
752 recognize five subfamilies within Amaranthaceae s.l. represented by the five well-supported  
753 major clades recovered in this study (Fig. 2): Amaranthoideae (Amaranthaceae s.s.), Betoideae,  
754 Chenopodioideae ('Chenopods I'), Polycnemoideae, and Salicornioideae ('Chenopods II').

755

### 756 *Conclusions*

757 Our analyses highlight the need to test for multiple sources of conflict in phylogenomic  
758 analyses, especially when trying to resolve phylogenetic relationships with extensive  
759 phylogenetic conflict. Furthermore, one needs to be aware of the strengths and limitations of

760 different phylogenetic methods and be cautious about relying on any single analysis, for example  
761 in the usage of phylogenetics species networks over coalescent-based species trees (Blair and  
762 Ané 2020). We make the following recommendation on five essential steps towards exploring  
763 heterogeneous phylogenetic signals in phylogenomic datasets in general. 1) Study design:  
764 consider whether the taxon sampling and marker choice enable testing alternative sources of  
765 conflicting phylogenetic signal. For example, will there be sufficient phylogenetic signal and  
766 sufficient taxon coverage in individual gene trees for methods such as phylogenetic network  
767 analyses? 2) Data processing: care should be taken in data cleaning, partitioning (e.g., nuclear vs.  
768 plastid), and using orthology inference methods that explicitly address paralogy issues (e.g., tree-  
769 based orthology inference and synteny information). 3) Species tree inference: select species tree  
770 methods that accommodate the dataset size and data type (e.g., ASTRAL for gene tree-based  
771 inferences or SVDquartet [Chifman and Kubatko 2014] for SNP-based inferences), followed by  
772 visualization of phylogenetic conflict using tools such as the pie charts (e.g., PhyParts) and  
773 quartet-based tools (e.g., Quartet Sampling; Quadripartition Internode Certainty [Zhou et al.  
774 2020]; Concordance Factors [Minh et al. 2020]). 4) Assessing hybridization: if phylogenetic  
775 conflict cannot be explained by processes like ILS, phylogenetic species network analyses (e.g.,  
776 PhyloNet) reduced taxon sampling can be applied to test hybridization hypotheses given results  
777 in step 3; 5) Hypothesis testing: additional tests can be performed given the results of  
778 recommendation 3 and 4 and depending on the scenario. These could include testing for model  
779 misspecification, anomaly zone, uninformative gene tree, and if hybridization is hypothesized,  
780 testing putative reticulation events one at a time, as illustrated in this study.

781         Despite using genome-scale data and exhaustive hypothesis testing, the backbone  
782 phylogeny of Amaranthaceae s.l. remains unresolved, and we were unable to distinguish ancient

783 hybridization events from ILS or uninformative gene trees. Similar situations might not be  
784 atypical across the Tree of Life. As we leverage more genomic data and explore gene tree  
785 discordance in more detail, these steps will be informative in other clades, especially in those  
786 that are products of ancient and rapid lineage diversification (e.g., Widhelm et al. 2019; Koenen  
787 et al. 2020). Ultimately, such endeavors will be instrumental in gaining a full understanding of  
788 the complexity of the Tree of Life.

789

790

#### SUPPLEMENTARY MATERIAL

791 Data available from the Dryad Digital Repository: [http://dx.doi.org/10.5061/.\[NNNN\]](http://dx.doi.org/10.5061/.[NNNN])

792

793

#### ACKNOWLEDGMENTS

794 The authors thank H. Freitag, J.M. Bena and the Millennium Seed Bank for providing seeds; U.  
795 Martiné for assisting with RNA extraction; N. Wang and Y.-Y. Huang for sample sequencing. A.  
796 Crum, R. Ree, B. Carstens, and three anonymous reviewers for providing helpful comments; the  
797 Minnesota Supercomputing Institute (MSI) at the University of Minnesota for providing access  
798 to computational resources. This work was supported by the University of Minnesota, the  
799 University of Michigan, the US National Science Foundation (DEB 1354048), and the  
800 Department of Energy, Office of Science, Genomic Science Program (Contract Number DE-  
801 SC0008834).

802

803

**REFERENCES**

804

Alda F., Tagliacollo V.A., Bernt M.J., Waltz B.T., Ludt W.B., Faircloth B.C., Alfaro M.E.,

805

Albert J.S., Chakrabarty P. 2019. Resolving Deep Nodes in an Ancient Radiation of

806

Neotropical Fishes in the Presence of Conflicting Signals from Incomplete Lineage

807

Sorting. *Syst. Biol.* 68:573–593.

808

Bankevich A., Nurk S., Antipov D., Gurevich A.A., Dvorkin M., Kulikov A.S., Lesin V.M.,

809

Nikolenko S.I., Pham S., Prjibelski A.D., Pyshkin A.V., Sirotkin A.V., Vyahhi N., Tesler

810

G., Alekseyev M.A., Pevzner P.A. 2012. SPAdes: A New Genome Assembly Algorithm

811

and Its Applications to Single-Cell Sequencing. *J. Comput. Biol.* 19:455–477.

812

Bena M.J., Acosta J.M., Aagesen L. 2017. Macroclimatic niche limits and the evolution of C<sub>4</sub>

813

photosynthesis in Gomphrenoideae (Amaranthaceae). *Bot. J. Linn. Soc.* 184:283–297.

814

Blackmon H., Adams R.A. 2015 EvobiR: Tools for comparative analyses and teaching

815

evolutionary biology. doi:10.5281/zenodo.30938

816

Blair C., Ané C. 2020. Phylogenetic Trees and Networks Can Serve as Powerful and

817

Complementary Approaches for Analysis of Genomic Data. *Syst. Biol.* 69:593–601.

818

Bouckaert R., Heled J. 2014. DensiTree 2: Seeing Trees Through the Forest. *BioRxiv.* 012401.

819

Brown J.W., Walker J.F., Smith S.A. 2017. Phyx - phylogenetic tools for unix. *Bioinformatics.*

820

33:1886–1888.

821

Bruen T.C., Philippe H., Bryant D. 2006. A Simple and Robust Statistical Test for Detecting the

822

Presence of Recombination. *Genetics.* 172:2665–2681.

823

Buckley T.R., Cordeiro M., Marshall D.C., Simon C. 2006. Differentiating between Hypotheses

824

of Lineage Sorting and Introgression in New Zealand Alpine Cicadas (Maoricicada

825

Dugdale). *Syst. Biol.* 55:411–425.

- 826 Chen L.-Y., Morales-Briones D.F., Passow C.N., Yang Y. 2019. Performance of gene expression  
827 analyses using de novo assembled transcripts in polyploid species. *Bioinformatics*.  
828 35:4314–4320.
- 829 Chifman J., Kubatko L. 2014. Quartet Inference from SNP Data Under the Coalescent Model.  
830 *Bioinformatics*. 30:3317–3324.
- 831 Cloutier A., Sackton T.B., Grayson P., Clamp M., Baker A.J., Edwards S.V. 2019. Whole-  
832 Genome Analyses Resolve the Phylogeny of Flightless Birds (Palaeognathae) in the  
833 Presence of an Empirical Anomaly Zone. *Syst. Biol.* 68:937–955
- 834 Cooper E.D. 2014. Overly simplistic substitution models obscure green plant phylogeny. *Trends*  
835 *Plant Sci.* 19:576–582.
- 836 Copetti D., Búrquez A., Bustamante E., Charboneau J.L.M., Childs K.L., Eguiarte L.E., Lee S.,  
837 Liu T.L., McMahon M.M., Whiteman N.K., Wing R.A., Wojciechowski M.F., Sanderson  
838 M.J. 2017. Extensive gene tree discordance and hemiplasy shaped the genomes of North  
839 American columnar cacti. *Proc. Natl. Acad. Sci.* 114:12003–12008.
- 840 Cox C.J., Li B., Foster P.G., Embley T.M., Civián P. 2014. Conflicting Phylogenies for Early  
841 Land Plants are Caused by Composition Biases among Synonymous Substitutions. *Syst.*  
842 *Biol.* 63:272–279.
- 843 Crowl A.A., Manos P.S., McVay J.D., Lemmon A.R., Lemmon E.M., Hipp A.L. 2020.  
844 Uncovering the genomic signature of ancient introgression between white oak lineages  
845 (*Quercus*). *New Phytol.* 226:1158–1170.
- 846 Davidson N.M., Oshlack A. 2014. Corset: enabling differential gene expression analysis for de  
847 novo assembled transcriptomes. *Genome Biol.* 15:57.

- 848 Degnan J.H., Rosenberg N.A. 2006. Discordance of Species Trees with Their Most Likely Gene  
849 Trees. *PLoS Genet.* 2:e68.
- 850 Degnan J.H., Rosenberg N.A. 2009. Gene tree discordance, phylogenetic inference and the  
851 multispecies coalescent. *Trends Ecol. Evol.* 24:332–340.
- 852 Di Vincenzo V., Gruenstaeudl M., Nauheimer L., Wondafrash M., Kamau P., Demissew S.,  
853 Borsch T. 2018. Evolutionary diversification of the African achyranthoid clade  
854 (Amaranthaceae) in the context of sterile flower evolution and epizoochory. *Ann. Bot.*  
855 122:69–85.
- 856 Dohm J.C., Minoche A.E., Holtgräwe D., Capella-Gutiérrez S., Zakrzewski F., Tafer H., Rupp  
857 O., Sörensen T.R., Stracke R., Reinhardt R., Goesmann A., Kraft T., Schulz B., Stadler  
858 P.F., Schmidt T., Gabaldón T., Lehrach H., Weisshaar B., Himmelbauer H. 2014. The  
859 genome of the recently domesticated crop plant sugar beet (*Beta vulgaris*). *Nature.*  
860 505:546–549.
- 861 Doyle J.J. 1992. Gene Trees and Species Trees: Molecular Systematics as One-Character  
862 Taxonomy. *Syst. Bot.* 17:144.
- 863 Durand E.Y., Patterson N., Reich D., Slatkin M. 2011. Testing for Ancient Admixture between  
864 Closely Related Populations. *Mol. Biol. Evol.* 28:2239–2252.
- 865 Edwards S.V. 2009. Is A New and General Theory of Molecular Systematics Emerging?  
866 *Evolution.* 63:1–19.
- 867 Edwards S.V., Xi Z., Janke A., Faircloth B.C., McCormack J.E., Glenn T.C., Zhong B., Wu S.,  
868 Lemmon E.M., Lemmon A.R., Leaché A.D., Liu L., Davis C.C. 2016. Implementing and  
869 testing the multispecies coalescent model: A valuable paradigm for phylogenomics. *Mol.*  
870 *Phylogenet. Evol.* 94:447–462.



- 871 Elworth R.A.L., Allen C., Benedict T., Dulworth P., Nakhleh L.K. 2018. DGEN: A Test Statistic  
872 for Detection of General Introgression Scenarios. WABI.
- 873 Elworth R.A.L., Ogilvie H.A., Zhu J., Nakhleh L. 2019. Advances in Computational Methods for  
874 Phylogenetic Networks in the Presence of Hybridization. In: Warnow T., editor.  
875 Bioinformatics and Phylogenetics: Seminal Contributions of Bernard Moret. Cham:  
876 Springer International Publishing. p. 317–360.
- 877 Erfan Sayyari, Siavash Mirarab. 2018. Testing for Polytomies in Phylogenetic Species Trees  
878 Using Quartet Frequencies. *Genes*. 9:132.
- 879 Flowers T.J., Colmer T.D. 2015. Plant salt tolerance: adaptations in halophytes. *Ann. Bot.*  
880 115:327–331.
- 881 Folk R.A., Mandel J.R., Freudenstein J.V. 2017. Ancestral Gene Flow and Parallel Organellar  
882 Genome Capture Result in Extreme Phylogenomic Discord in a Lineage of Angiosperms.  
883 *Syst. Biol.* 66:320-337.
- 884 Fontaine M.C., Pease J.B., Steele A., Waterhouse R.M., Neafsey D.E., Sharakhov I.V., Jiang X.,  
885 Hall A.B., Catteruccia F., Kakani E., Mitchell S.N., Wu Y.-C., Smith H.A., Love R.R.,  
886 Lawniczak M.K., Slotman M.A., Emrich S.J., Hahn M.W., Besansky N.J. 2015.  
887 Extensive introgression in a malaria vector species complex revealed by phylogenomics.  
888 *Science*. 347:1258524.
- 889 Foster P.G. 2004. Modeling Compositional Heterogeneity. *Syst. Biol.* 53:485–495.
- 890 Galtier N., Daubin V. 2008. Dealing with incongruence in phylogenomic analyses. *Philos. Trans.*  
891 *R. Soc. B Biol. Sci.* 363:4023–4029.

- 892 Gitzendanner M.A., Soltis P.S., Yi T.-S., Li D.-Z., Soltis D.E. 2018. Plastome Phylogenetics: 30  
893 Years of Inferences Into Plant Evolution. *Plastid Genome Evolution*. Elsevier. p. 293–  
894 313.
- 895 Gonçalves D.J.P., Simpson B.B., Ortiz E.M., Shimizu G.H., Jansen R.K. 2019. Incongruence  
896 between gene trees and species trees and phylogenetic signal variation in plastid genes.  
897 *Mol. Phylogenet. Evol.* 138:219–232.
- 898 Grabherr M.G., Haas B.J., Yassour M., Levin J.Z., Thompson D.A., Amit I., Adiconis X., Fan  
899 L., Raychowdhury R., Zeng Q., Chen Z., Mauceli E., Hacohen N., Gnirke A., Rhind N.,  
900 di Palma F., Birren B.W., Nusbaum C., Lindblad-Toh K., Friedman N., Regev A. 2011.  
901 Full-length transcriptome assembly from RNA-Seq data without a reference genome.  
902 *Nat. Biotechnol.* 29:644–652.
- 903 Green R.E., Krause J., Briggs A.W., Maricic T., Stenzel U., Kircher M., Patterson N., Li H., Zhai  
904 W., Fritz M.H.Y., Hansen N.F., Durand E.Y., Malaspina A.S., Jensen J.D., Marques-  
905 Bonet T., Alkan C., Prufer K., Meyer M., Burbano H.A., Good J.M., Schultz R., Aximu-  
906 Petri A., Butthof A., Hober B., Hoffner B., Siegemund M., Weihmann A., Nusbaum C.,  
907 Lander E.S., Russ C., Novod N., Affourtit J., Egholm M., Verna C., Rudan P., Brajkovic  
908 D., Kucan Z., Gusic I., Doronichev V.B., Golovanova L.V., Lalueza-Fox C., de la Rasilla  
909 M., Fortea J., Rosas A., Schmitz R.W., Johnson P.L.F., Eichler E.E., Falush D., Birney  
910 E., Mullikin J.C., Slatkin M., Nielsen R., Kelso J., Lachmann M., Reich D., Paabo S.  
911 2010. A Draft Sequence of the Neandertal Genome. *Science.* 328:710–722.
- 912 Hejase H.A., Liu K.J. 2016. A scalability study of phylogenetic network inference methods using  
913 empirical datasets and simulations involving a single reticulation. *BMC Bioinformatics.*  
914 17:422.

- 915 Hejase H.A., VandePol N., Bonito G.M., Liu K.J. 2018. FastNet: Fast and Accurate Statistical  
916 Inference of Phylogenetic Networks Using Large-Scale Genomic Sequence Data. *Comp.*  
917 *Genomics.*:242–259.
- 918 Hernández-Ledesma P., Berendsohn W.G., Borsch T., Mering S.V., Akhiani H., Arias S.,  
919 Castañeda-Noa I., Eggli U., Eriksson R., Flores-Olvera H., Fuentes-Bazán S., Kadereit  
920 G., Klak C., Korotkova N., Nyffeler R., Ocampo G., Ochoterena H., Oxelman B.,  
921 Rabeler R.K., Sanchez A., Schlumpberger B.O., Uotila P. 2015. A taxonomic backbone  
922 for the global synthesis of species diversity in the angiosperm order Caryophyllales.  
923 *Willdenowia.* 45:281.
- 924 Hoang D.T., Chernomor O. 2018. UFBoot2: Improving the Ultrafast Bootstrap Approximation.  
925 *Mol. Biol. Evol.* 35:518–522.
- 926 Hohmann S., Kadereit J.W., Kadereit G. 2006. Understanding Mediterranean-Californian  
927 disjunctions: molecular evidence from Chenopodiaceae-Betoideae. *TAXON.* 55:67–78.
- 928 Holder M.T., Anderson J.A., Holloway A.K. 2001. Difficulties in Detecting Hybridization. *Syst.*  
929 *Biol.* 50:978–982.
- 930 Huang H., Knowles L.L. 2009. What Is the Danger of the Anomaly Zone for Empirical  
931 Phylogenetics? *Syst. Biol.* 58:527–536.
- 932 Huang W., Zhou G., Marchand M., Ash J.R., Morris D., Van Dooren P., Brown J.M., Gallivan  
933 K.A., Wilgenbusch J.C. 2016. TreeScaper: Visualizing and Extracting Phylogenetic  
934 Signal from Sets of Trees. *Mol. Biol. Evol.* 33:3314–3316.
- 935 Jarvis D.E., Ho Y.S., Lightfoot D.J., Schmöckel S.M., Li B., Borm T.J.A., Ohyanagi H., Mineta  
936 K., Michell C.T., Saber N., Kharbatia N.M., Rupper R.R., Sharp A.R., Dally N.,  
937 Boughton B.A., Woo Y.H., Gao G., Schijlen E.G.W.M., Guo X., Momin A.A., Negrão

- 938 S., Al-Babili S., Gehring C., Roessner U., Jung C., Murphy K., Arold S.T., Gojobori T.,  
939 Linden C.G.V.D., van Loo E.N., Jellen E.N., Maughan P.J., Tester M. 2017. The genome  
940 of *Chenopodium quinoa*. *Nature*. 542:307–312.
- 941 Kadereit G., Ackerly D., Pirie M.D. 2012. A broader model for C<sub>4</sub> photosynthesis evolution in  
942 plants inferred from the goosefoot family (Chenopodiaceae s.s.). *Proc. R. Soc. B Biol.*  
943 *Sci.* 279:3304–3311.
- 944 Kadereit G., Borsch T., Weising K., Freitag H. 2003. Phylogeny of Amaranthaceae and  
945 Chenopodiaceae and the Evolution of C<sub>4</sub> Photosynthesis. *Int. J. Plant Sci.* 164:959–986.
- 946 Kadereit G., Hohmann S., Kadereit J.W. 2006. A synopsis of Chenopodiaceae subfam. Betoideae  
947 and notes on the taxonomy of *Beta*. *Willdenowia*. 36:9–19.
- 948 Kadereit G., Newton R.J., Vandeloek F. 2017. Evolutionary ecology of fast seed germination—  
949 A case study in Amaranthaceae/Chenopodiaceae. *Perspect. Plant Ecol. Evol. Syst.* 29:1–  
950 11.
- 951 Kalyaanamoorthy S., Minh B.Q., Wong T.K.F., von Haeseler A., Jermiin L.S. 2017.  
952 ModelFinder: fast model selection for accurate phylogenetic estimates. *Nat. Methods*.  
953 14:587–589.
- 954 Kamneva O.K., Rosenberg N.A. 2017. Simulation-Based Evaluation of Hybridization Network  
955 Reconstruction Methods in the Presence of Incomplete Lineage Sorting. *Evol.*  
956 *Bioinforma.* 13:117693431769193.
- 957 Katoh K., Standley D.M. 2013. MAFFT Multiple Sequence Alignment Software Version 7:  
958 Improvements in Performance and Usability. *Mol. Biol. Evol.* 30:772–780.
- 959 Kearse M., Moir R., Wilson A., Stones-Havas S., Cheung M., Sturrock S., Buxton S., Cooper A.,  
960 Markowitz S., Duran C., Thierer T., Ashton B., Meintjes P., Drummond A. 2012.

- 961 Geneious Basic: An integrated and extendable desktop software platform for the  
962 organization and analysis of sequence data. *Bioinformatics*. 28:1647–1649.
- 963 Knowles L.L., Huang H., Sukumaran J., Smith S.A. 2018. A matter of phylogenetic scale:  
964 Distinguishing incomplete lineage sorting from lateral gene transfer as the cause of gene  
965 tree discord in recent versus deep diversification histories. *Am. J. Bot.* 105:376–384.
- 966 Koenen, E., Ojeda, D., Steeves, R., Migliore, J., Bakker, F., Wieringa, J., Kidner, C., Hardy, O.,  
967 Pennington, R., Bruneau, A., Hughes, C. 2020. Large-scale genomic sequence data  
968 resolve the deepest divergences in the legume phylogeny and support a near-  
969 simultaneous evolutionary origin of all six subfamilies. *New Phytol.* 225: 1355-1369.
- 970 Kubatko L.S., Chifman J. 2019. An invariants-based method for efficient identification of hybrid  
971 species from large-scale genomic data. *BMC Evol. Biol.* 19:112.
- 972 Kumar, S., Filipski, A., Battistuzzi, F., Kosakovsky Pond, S., Tamura, K., 2012. Statistics and  
973 truth in phylogenomics. *Mol. Biol. Evol.* 29:457–472.
- 974 Lanfear R., Calcott B., Ho S.Y.W., Guindon S. 2012. PartitionFinder: Combined Selection of  
975 Partitioning Schemes and Substitution Models for Phylogenetic Analyses. *Mol. Biol.*  
976 *Evol.* 29:1695–1701.
- 977 Lee-Yaw J.A., Grassa C.J., Joly S., Andrew R.L., Rieseberg L.H. 2019. An evaluation of  
978 alternative explanations for widespread cytonuclear discordance in annual sunflowers  
979 (*Helianthus*). *New Phytol.* 221:515–526.
- 980 Li, B., Wang, J., Yao, L., Meng, Y., Ma, X., Si, E., Ren, P., Yang, K., Shang, X., Wang, H.  
981 Halophyte *Halogeton glomeratus*, a promising candidate for phytoremediation of heavy  
982 metal-contaminated saline soils. *Plant Soil.* 442:323–331.

- 983 Lightfoot D.J., Jarvis D.E., Ramaraj T., Lee R., Jellen E.N., Maughan P.J. 2017. Single-molecule  
984 sequencing and Hi-C-based proximity-guided assembly of amaranth (*Amaranthus*  
985 *hypochondriacus*) chromosomes provide insights into genome evolution. BMC Biol.  
986 15:74.
- 987 Linkem C.W., Minin V.N., Leaché A.D. 2016. Detecting the Anomaly Zone in Species Trees  
988 and Evidence for a Misleading Signal in Higher-Level Skink Phylogeny (Squamata:  
989 Scincidae). Syst. Biol. 65:465–477.
- 990 Liu L., Yu L. 2010. Phybase: an R package for species tree analysis. Bioinformatics. 26:962–  
991 963.
- 992 Liu Y., Cox C.J., Wang W., Goffinet B. 2014. Mitochondrial Phylogenomics of Early Land  
993 Plants: Mitigating the Effects of Saturation, Compositional Heterogeneity, and Codon-  
994 Usage Bias. Syst. Biol. 63:862–878.
- 995 Maddison W.P. 1997. Gene Trees in Species Trees. Syst. Biol. 46:532–536.
- 996 Masson R., Kadereit G. 2013. Phylogeny of Polycnemoideae (Amaranthaceae): Implications for  
997 biogeography, character evolution and taxonomy. TAXON. 62:100–111.
- 998 Maureira-Butler I.J., Pfeil B.E., Muangprom A., Osborn T.C., Doyle J.J. 2008. The Reticulate  
999 History of *Medicago* (Fabaceae). Syst. Biol. 57:466–482.
- 1000 Mclean B.S., Bell K.C., Allen J.M., Helgen K.M., Cook J.A. 2019. Impacts of Inference Method  
1001 and Data set Filtering on Phylogenomic Resolution in a Rapid Radiation of Ground  
1002 Squirrels (Xerinae: Marmotini). Syst. Biol. 68:298–316.
- 1003 Meyer B.S., Matschiner M., Salzburger W. 2017. Disentangling Incomplete Lineage Sorting and  
1004 Introgression to Refine Species-Tree Estimates for Lake Tanganyika Cichlid Fishes. Syst.  
1005 Biol. 66:531–550.

- 1006 Minh B.Q., Hahn M., Lanfear R. 2020. New methods to calculate concordance factors for  
1007 phylogenomic datasets. *Mol. Biol. Evol.* msaa106
- 1008 Mirarab S., Bayzid M.S., Warnow T. 2016. Evaluating Summary Methods for Multilocus  
1009 Species Tree Estimation in the Presence of Incomplete Lineage Sorting. *Syst. Biol.*  
1010 65:366–380.
- 1011 Morales-Briones D.F., Liston A., Tank D.C. 2018a. Phylogenomic analyses reveal a deep history  
1012 of hybridization and polyploidy in the Neotropical genus *Lachemilla* (Rosaceae). *New*  
1013 *Phytol.* 218:1668–1684.
- 1014 Morales-Briones D.F., Romoleroux K., Kolář F., Tank D.C. 2018b. Phylogeny and Evolution of  
1015 the Neotropical Radiation of *Lachemilla* (Rosaceae): Uncovering a History of Reticulate  
1016 Evolution and Implications for Infrageneric Classification. *Syst. Bot.* 43:17–34.
- 1017 Moray C., Goolsby E.W., Bromham L. 2016. The Phylogenetic Association Between Salt  
1018 Tolerance and Heavy Metal Hyperaccumulation in Angiosperms. *Evol. Biol.* 43:119–  
1019 130.
- 1020 Mower J.P. 2009. The PREP suite: predictive RNA editors for plant mitochondrial genes,  
1021 chloroplast genes and user-defined alignments. *Nucleic Acids Res.* 37:W253–W259.
- 1022 Müller K., Borsch T. 2005. Phylogenetics of Amaranthaceae Based on *matK/trnK* Sequence  
1023 Data: Evidence from Parsimony, Likelihood, and Bayesian Analyses. *Ann. Mo. Bot.*  
1024 *Gard.* 92:66–102.
- 1025 Nguyen L.-T., Schmidt H.A., von Haeseler A., Minh B.Q. 2015. IQ-TREE: A Fast and Effective  
1026 Stochastic Algorithm for Estimating Maximum-Likelihood Phylogenies. *Mol. Biol. Evol.*  
1027 32:268–274.

- 1028 Osuna-Mascaró C., Rubio de Casas R., Perfectti F. 2018. Comparative assessment shows the  
1029 reliability of chloroplast genome assembly using RNA-seq. *Sci. Rep.* 8:17404.
- 1030 Pamilo P., Nei M. 1988. Relationships between Gene Trees and Species Trees. *Mol. Biol. Evol.*  
1031 5:568–583.
- 1032 Pease J.B., Brown J.W., Walker J.F., Hinchliff C.E., Smith S.A. 2018. Quartet Sampling  
1033 distinguishes lack of support from conflicting support in the green plant tree of life. *Am.*  
1034 *J. Bot.* 105:385–403.
- 1035 Piirainen M., Liebisch O., Kadereit G. 2017. Phylogeny, biogeography, systematics and  
1036 taxonomy of Salicornioideae (Amaranthaceae/Chenopodiaceae) – A cosmopolitan, highly  
1037 specialized hygrohalophyte lineage dating back to the Oligocene. *Taxon.* 66:109–132.
- 1038 Prasanna A.N., Gerber D., Kijpornyongpan T., Aime M.C., Doyle V.P., Nagy L.G. 2020. Model  
1039 Choice, Missing Data, and Taxon Sampling Impact Phylogenomic Inference of Deep  
1040 Basidiomycota Relationships. 69:17–37
- 1041 R Core Team. 2019. R: A Language and Environment for Statistical Computing. Vienna,  
1042 Austria: R Foundation for Statistical Computing.
- 1043 Rannala B., Yang Z. 2003. Bayes Estimation of Species Divergence Times and Ancestral  
1044 Population Sizes Using DNA Sequences From Multiple Loci. *Genetics.* 166:1645–1656.
- 1045 Rieseberg L.H., Soltis D.E. 1991. Phylogenetic consequences of cytoplasmic gene flow in plants.  
1046 *Evol. Trends Plants.* 5:65–84.
- 1047 Robinson D.F., Foulds L.R. 1981. Comparison of phylogenetic trees. *Math. Biosci.* 53:131–147.
- 1048 Rosenberg N.A. 2013. Discordance of Species Trees with Their Most Likely Gene Trees: A  
1049 Unifying Principle. *Mol. Biol. Evol.* 30:2709–2713.



- 1050 Roycroft E.J., Moussalli A., Rowe K.C. 2020. Phylogenomics Uncovers Confidence and  
1051 Conflict in the Rapid Radiation of Australo-Papuan Rodents. *Syst. Biol.* 69:431–444.
- 1052 Salichos L., Stamatakis A., Rokas A. 2014. Novel Information Theory-Based Measures for  
1053 Quantifying Incongruence among Phylogenetic Trees. *Mol. Biol. Evol.* 31:1261–1271.
- 1054 Sang T., Crawford D.J., Stuessy T.F. 1995. Documentation of reticulate evolution in peonies  
1055 (*Paeonia*) using internal transcribed spacer sequences of nuclear ribosomal DNA:  
1056 implications for biogeography and concerted evolution. *Proc. Natl. Acad. Sci.* 92:6813–  
1057 6817.
- 1058 Sayyari E., Mirarab S. 2016. Fast Coalescent-Based Computation of Local Branch Support from  
1059 Quartet Frequencies. *Mol. Biol. Evol.* 33:1654–1668.
- 1060 Schliep K.P. 2011. phangorn: phylogenetic analysis in R. *Bioinformatics.* 27:592–593.
- 1061 Schliesky S., Gowik U., Weber A.P.M., Bräutigam A. 2012. RNA-Seq Assembly – Are We  
1062 There Yet? *Front. Plant Sci.* 3:220.
- 1063 Schwarz G. 1978. Estimating the Dimension of a Model. *Ann. Stat.* 6:461–464.
- 1064 Sharp P.M., Li W.-H. 1986. An evolutionary perspective on synonymous codon usage in  
1065 unicellular organisms. *J. Mol. Evol.* 24:28–38.
- 1066 Shi C., Wang S., Xia E.-H., Jiang J.-J., Zeng F.-C., Gao L.-Z. 2016. Full transcription of the  
1067 chloroplast genome in photosynthetic eukaryotes. *Sci. Rep.* 6:30135.
- 1068 Shimodaira H. 2002. An Approximately Unbiased Test of Phylogenetic Tree Selection. *Syst.*  
1069 *Biol.* 51:492–508.
- 1070 Shimodaira H., Hasegawa M. 2001. CONSEL: for assessing the confidence of phylogenetic tree  
1071 selection. *Bioinformatics.* 17:1246–1247.

- 1072 Smith D.R. 2013. RNA-Seq data: a goldmine for organelle research. *Brief. Funct. Genomics*.  
1073 12:454–456.
- 1074 Smith S.A., Moore M.J., Brown J.W., Yang Y. 2015. Analysis of phylogenomic datasets reveals  
1075 conflict, concordance, and gene duplications with examples from animals and plants.  
1076 *BMC Evol. Biol.* 15:745.
- 1077 Smith S.A., O’Meara B.C. 2012. treePL: divergence time estimation using penalized likelihood  
1078 for large phylogenies. *Bioinformatics*. 28:2689–2690.
- 1079 Solís-Lemus C., Ané C. 2016a. Inferring Phylogenetic Networks with Maximum  
1080 Pseudolikelihood under Incomplete Lineage Sorting. *PLOS Genet.* 12:e1005896.
- 1081 Soltis D.E., Kuzoff R.K. 1995. Discordance between nuclear and chloroplast phylogenies in the  
1082 *Heuchera* group (Saxifragaceae). *Evolution*. 49:727–742.
- 1083 Srivastava S.K. 1969. Assorted angiosperm pollen from the Edmonton Formation  
1084 (Maestrichtian), Alberta, Canada. *Can. J. Bot.* 47:975–989.
- 1085 Stamatakis A. 2014. RAxML version 8 - a tool for phylogenetic analysis and post-analysis of  
1086 large phylogenies. *Bioinformatics*. 30:1312–1313.
- 1087 Sugiura N. 1978. Further analysts of the data by akaike’ s information criterion and the finite  
1088 corrections. *Commun. Stat. - Theory Methods*. 7:13–26.
- 1089 Swofford D. 2002. PAUP\*. Phylogenetic analysis using parsimony (\*and other methods) version  
1090 4. Sunderland MA Sinauer Assoc.
- 1091 Than C., Ruths D., Nakhleh L. 2008. PhyloNet: a software package for analyzing and  
1092 reconstructing reticulate evolutionary relationships. *BMC Bioinformatics*. 9:322–16.
- 1093 The Angiosperm Phylogeny Group, Chase M.W., Christenhusz M.J.M., Fay M.F., Byng J.W.,  
1094 Judd W.S., Soltis D.E., Mabberley D.J., Sennikov A.N., Soltis P.S., Stevens P.F. 2016.

- 1095 An update of the Angiosperm Phylogeny Group classification for the orders and families  
1096 of flowering plants: APG IV. *Bot. J. Linn. Soc.* 181:1–20.
- 1097 Vargas O.M., Ortiz E.M., Simpson B.B. 2017. Conflicting phylogenomic signals reveal a pattern  
1098 of reticulate evolution in a recent high-Andean diversification (Asteraceae: Astereae:  
1099 *Diplostephium*). *New Phytol.* 214:1736–1750.
- 1100 Walker J.F., Walker-Hale N., Vargas O.M., Larson D.A., Stull G.W. 2019. Characterizing gene  
1101 tree conflict in plastome-inferred phylogenies. *PeerJ.* 7:e7747.
- 1102 Walker J.F., Yang Y., Feng T., Timoneda A., Mikenas J., Hutchison V., Edwards C., Wang N.,  
1103 Ahluwalia S., Olivieri J., Walker-Hale N., Majure L.C., Puente R., Kadereit G.,  
1104 Lauterbach M., Eggli U., Flores-Olvera H., Ochoterena H., Brockington S.F., Moore  
1105 M.J., Smith S.A. 2018. From cacti to carnivores: Improved phylotranscriptomic sampling  
1106 and hierarchical homology inference provide further insight into the evolution of  
1107 Caryophyllales. *Am. J. Bot.* 105:446–462.
- 1108 Wen D., Yu Y., Hahn M.W., Nakhleh L. 2016. Reticulate evolutionary history and extensive  
1109 introgression in mosquito species revealed by phylogenetic network analysis. *Mol. Ecol.*  
1110 25:2361–2372.
- 1111 Wen D., Yu Y., Zhu J., Nakhleh L. 2018. Inferring Phylogenetic Networks Using PhyloNet.  
1112 *Syst. Biol.* 67:735–740.
- 1113 Widhalm T.J., Grewe F., Huang J.-P., Mercado-Díaz J.A., Goffinet B., Lücking R., Moncada B.,  
1114 Mason-Gamer R., Lumbsch H.T. 2019. Multiple historical processes obscure  
1115 phylogenetic relationships in a taxonomically difficult group (Lobariaceae, Ascomycota).  
1116 *Sci. Rep.* 9:8968.

- 1117 Xu B., Yang Z. 2016. Challenges in Species Tree Estimation Under the Multispecies Coalescent  
1118 Model. *Genetics*. 204:1353–1368.
- 1119 Xu C., Jiao C., Sun H., Cai X., Wang X., Ge C., Zheng Y., Liu W., Sun X., Xu Y., Deng J.,  
1120 Zhang Z., Huang S., Dai S., Mou B., Wang Q., Fei Z., Wang Q. 2017. Draft genome of  
1121 spinach and transcriptome diversity of 120 *Spinacia* accessions. *Nat. Commun.* 8:15275.
- 1122 Yang Y., Moore M.J., Brockington S.F., Timoneda A., Feng T., Marx H.E., Walker J.F., Smith  
1123 S.A. 2017. An Efficient Field and Laboratory Workflow for Plant Phylotranscriptomic  
1124 Projects. *Appl. Plant Sci.* 5:1600128.
- 1125 Yang Y., Smith S.A. 2014. Orthology Inference in Nonmodel Organisms Using Transcriptomes  
1126 and Low-Coverage Genomes: Improving Accuracy and Matrix Occupancy for  
1127 Phylogenomics. *Mol. Biol. Evol.* 31:3081–3092.
- 1128 Yao G., Jin J.-J., Li H.-T., Yang J.-B., Mandala V.S., Croley M., Mostow R., Douglas N.A.,  
1129 Chase M.W., Christenhusz M.J.M., Soltis D.E., Soltis P.S., Smith S.A., Brockington S.F.,  
1130 Moore M.J., Yi T.-S., Li D.-Z. 2019. Plastid phylogenomic insights into the evolution of  
1131 Caryophyllales. *Mol. Phylogenet. Evol.* 134:74–86.
- 1132 Yu Y., Degnan J.H., Nakhleh L. 2012. The Probability of a Gene Tree Topology within a  
1133 Phylogenetic Network with Applications to Hybridization Detection. *PLoS Genet.*  
1134 8:e1002660–10.
- 1135 Yu Y., Dong J., Liu K.J., Nakhleh L. 2014. Maximum likelihood inference of reticulate  
1136 evolutionary histories. *Proc. Natl. Acad. Sci.* 111:16448–16453.
- 1137 Yu Y., Nakhleh L. 2015. A maximum pseudo-likelihood approach for phylogenetic networks.  
1138 *BMC Genomics.* 16:S10.

- 1139 Zhang C., Rabiee M., Sayyari E., Mirarab S. 2018. ASTRAL-III: polynomial time species tree  
1140 reconstruction from partially resolved gene trees. *BMC Bioinformatics*. 19:523.
- 1141 Zhao T., Schranz M.E. 2019. Network-based microsynteny analysis identifies major differences  
1142 and genomic outliers in mammalian and angiosperm genomes. *Proc. Natl. Acad. Sci.*  
1143 116:2165–2174.
- 1144 Zheng Y., Janke A. 2018. Gene flow analysis method, the D-statistic, is robust in a wide  
1145 parameter space. *BMC Bioinformatics*. 19:10.
- 1146 Zhou, X., Lutteropp, S., Czech, L., Stamatakis, A., Looz, M. V., Rokas, A. 2020. Quartet-based  
1147 computations of internode certainty provide robust measures of phylogenetic  
1148 incongruence. *Syst. Biol.* 69:308–324.
- 1149 Zhu J., Liu X., Ogilvie H.A., Nakhleh L.K. 2019. A divide-and-conquer method for scalable  
1150 phylogenetic network inference from multilocus data. *Bioinformatics*. 35:i370–i378.